International Journal of Earth Sciences
https://doi.org/10.1007/s00531-023-02353-y

ORIGINAL PAPER

An early Cambrian post-rift basin within the Baltica–Iapetus passive margin (north-central Scandinavian Caledonides)

Reinhard O. Greiling[1] · **Benno Kathol**[2,3] · **Risto A. Kumpulainen**[4]

Received: 2 May 2023 / Accepted: 25 September 2023

Abstract

Field data from recent geological mapping over a major part of the north-central Scandinavian Caledonides combined with published information give a detailed view of early Cambrian basin successions, comprising the Gärdsjön formation (Gf; Jämtland supergroup) in the Lower Allochthon and autochthonous equivalents (Dividal Group). The Gf comprises ten units of sandstone and siltstone or mudstone (Gf I—X, > 300 m thick). Green siltstones with red layers (Gf VI, c. 521 to 519 Ma) and green–grey siltstones at the top (Gf X, c. 516.5 to 513.5 Ma) are regional key horizons. Gf V, VI, VII, IX, and X deposition may be related to eustatic events. Restoration of Caledonian shortening reveals a major "Hornavan-Vattudal basin" (HVB; > 330 km NW–SE, > 400 km NE-SW) between the Grong–Olden culmination in the S and the Akkajaure–Tysfjord culmination in the N. Published zircon ages imply the latter separated the HVB from those shed from the Timan orogen in the N. The eastern basin margin straddles the present Caledonian erosional margin. Basement highs identified here within the Nasafjället, Bångonåive, and Børgefjellet "basement" windows define the western margin. They separate the HVB from the outer shelf towards the Iapetus Ocean in the W. The onset of sedimentation is time-related with E–W extension at c. 544–534 Ma. NNE–SSW-directed extension occurs after c. 518 Ma, perhaps related with Timan late-orogenic extension. The HVB is distinctly younger (c. 535–513.5 Ma) than Rodinia break-up and Iapetus ocean formation (> 550 Ma), comparable with post-rift basins in inner parts of modern passive margins.

Keywords Early Cambrian · Baltica passive margin · Post-rift basin · Syn-sedimentary faults · Restoration · Scandinavian Caledonides · Timan foreland

Introduction

In the wake of Rodinia break-up, Baltica developed passive continental margins in the (present) northwest and southwest, towards the Iapetus and Tornquist Oceans, respectively (Fig. 1a). Subsequent Baltica-Laurentia convergence and Caledonian shortening eventually led to nappe stacking into Lower, Middle, Upper, and Uppermost Allochthons beginning in Silurian times (e.g., Gee and Stephens 2020). As a result, these Caledonian nappes are now overlying the autochthonous, inner part of the north western Baltica passive margin (present orientation). Large-scale palinspastic restoration of Caledonian shortening (e.g., Andersen et al. 2022; Rice and Anderson 2016) shows the general geometry of the pre-Caledonian passive margin, mostly hyperextended towards the Iapetus Ocean. The traditional view of the sedimentary succession within the Baltica–Iapetus margin, now in the Lower and Middle Allochthons of the central Scandinavian Caledonides, comprises ocean

✉ Reinhard O. Greiling
r.o.greiling@kit.edu

Benno Kathol
Benno.Kathol@gmail.com

Risto A. Kumpulainen
Risto.Kumpulainen@geo.su.se

[1] Institute for Applied Geosciences, Structural Geology & Tectonophysics, Karlsruhe Institute of Technology (KIT), Adenauerring 20A, 76131 Karlsruhe, FR, Germany

[2] Geological Survey of Sweden, Box 670, 75128 Uppsala, Sweden

[3] Present Address: Sätunavägen 13D, 19546 Märsta, Sweden

[4] Department of Geological Sciences, Stockholm University, 106 91 Stockholm, Sweden

Published online: 19 October 2023

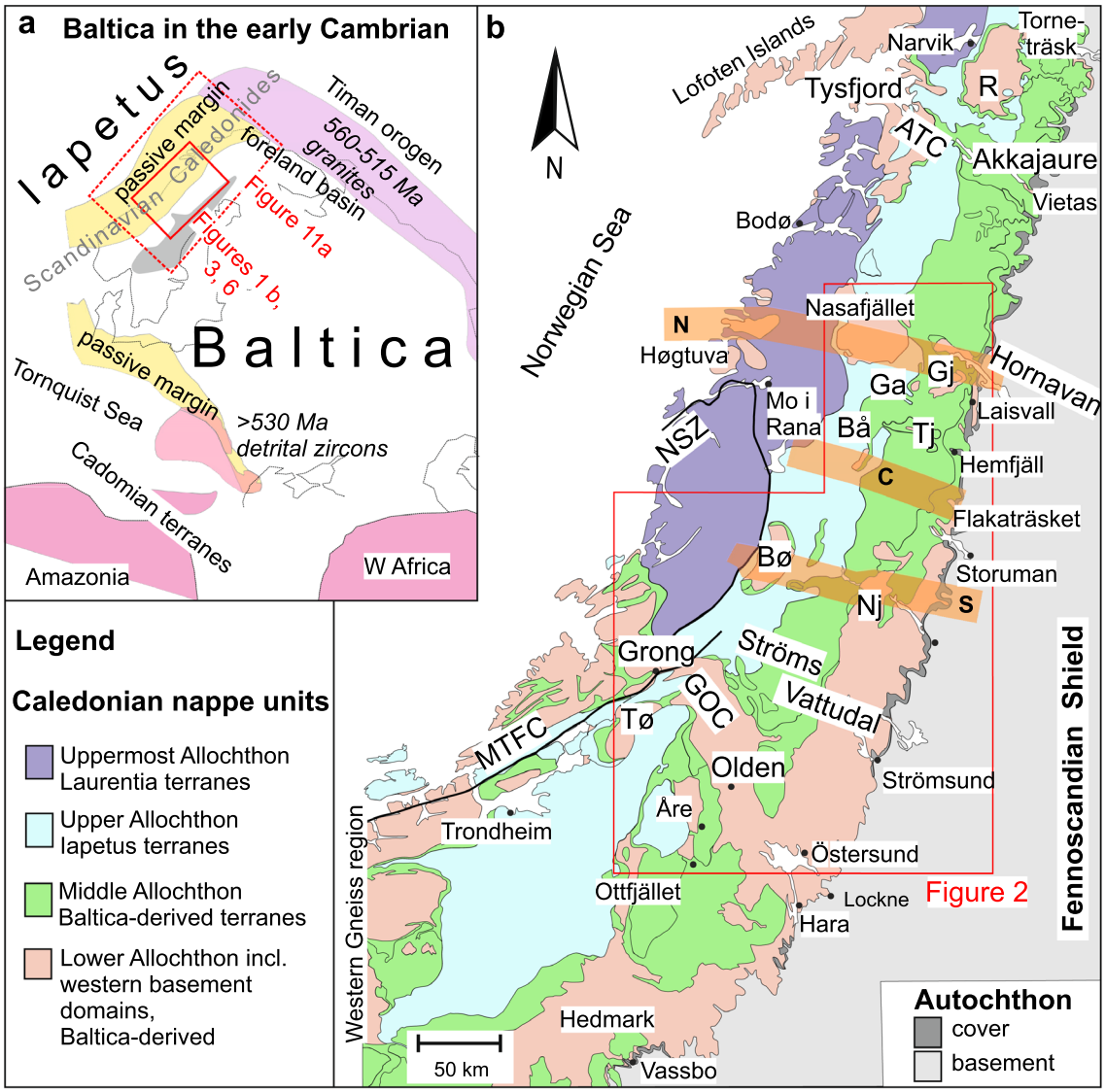

Fig. 1 **a** Baltica at the beginning of the Cambrian era with adjacent ocean basins and orogens, simplified from Pease et al. (2004), Johansson (2014), Slama and Pedersen (2015), Jakob et al. (2019), Żelaźniewicz et al. (2020). Early Cambrian land area in grey (Nielsen and Schovsbo 2011). **b** Geological sketch map of the central Scandinavian Caledonides, showing the studied area with three traverses documented in detail (orange stripes, N north, C central, S south; Figs. 6, 7). See Fig. 1a for location and Greiling et al. (2018) for sources. Møre-Trøndelag Fault Complex (MTFC) and Nesna Shear Zone (NSZ) simplified from Osmundsen et al. (2003). *ATC* Akkajaure–Tysfjord culmination, *Bå* Bångonåive window, *Bø* Børgefjellet window, *Ga* Gavas window, *Gj* Gautojaure area, *GOC* Grong-Olden culmination, *Nj* Njakafjället, *R* Rombak window, *Tj* Tjulån window, *Tø* Tømmerås window

ward-dipping and -thickening beds, spreading successively onto the developing Baltica passive margin in Neoproterozoic and Cambrian times (Jämtland supergroup, Gee and Kumpulainen 1980; Nielsen and Schovsbo 2011; Gee and Stephens 2020; SI Fig. S1). Structural complexities of the area's passive margin basins were documented in a limited area only (Gayer and Greiling 1989). Newly published evidence together with extensive field data of the authors shows a complex basin evolution of the Baltica passive margin in early Cambrian times. A substantial gap in time separates the lower Cambrian succession from underlying syn-rift beds and requires a revision of the earlier concepts. Towards that aim, this paper collects the available information from the relevant autochthonous and allochthonous (Lower Allochthon) units between the Akkajaure–Tysfjord– and Grong–Olden culminations (ATC, GOC; e.g., Björklund 1989; Gee and Stephens 2020; Fig. 1b). The new dataset comprises mainly detailed geological maps, field data, and new interpretations of comprehensive archive material from the Geological Survey of Sweden. Together with published age information, the new data allow correlations of the lower Cambrian units across the region, including the

autochthonous cover, and provide a base for a new view of the basin's geometry, subsidence history, evolution, and paleogeography. The discussion also puts the new results into the regional tectonic frame of the Baltica–Iapetus margin between the late Neoproterozoic-earliest Palaeozoic Timan orogen in the north (Pease et al. 2008) and the Cadomian terranes of similar age in the southeast (Żelaźniewicz et al. 2020; Fig. 1a). Most of the formations mentioned here lack definition according to the international standards (e.g., Kumpulainen et al. 2017). Therefore, no capital letter is used (e.g., Gärdsjön formation).

The sub-Cambrian basement

The basal unconformity of the Cambrian cover along the Caledonian erosional margin is almost flat at a regional scale ("sub-Cambrian peneplain"; e.g. Zachrisson and Greiling 1996; Lidmar-Bergström and Olmo 2015). At decimetre- to metre-levels, the basement surface shows a relief around Lake Storuman and in the Børgefjellet window (SI Fig. S2). In the Laisvall area, an observed basement relief (e.g., Lilljequist 1973; Willdén 1980) may be a product of tectonic activity (Saintilan et al. 2015). The crystalline basement is of Palaeoproterozoic age (Kathol and Weihed 2005; Bergman and Kathol 2018) and shows traces of weathering (Willdén 1980; Thelander 1982), for example disintegration of granite with isolated, kaolinized feldspar grains (e.g. Willdén 1980; SI Fig. S2) to a depth of a few metres beneath the Cambrian cover. Detailed studies on drill cores in the south of the area (Långviken, Hara) revealed weathering down to over 20 m beneath the basement–cover interface (Angerer and Greiling 2012). The basement displays numerous fractures of predominantly NW–SE and NNE–SSW directions (e.g. Bergman et al. 2012; Romer et al. 1994; Fig. 3). At the southern margin of the area, the Storsjön-Edsbyn Deformation Zone (Bergman et al. 2006) separates two distinct Palaeoproterozoic domains and may have influenced the Phanerozoic evolution (Olden Discontinuity Zone, ODZ, Bergman and Sjöström 1994). Mesoproterozoic mafic dykes (Greiling et al. 2007; Ripa and Stephens 2020) are mostly oriented NE–SW along the south-eastern Caledonian margin in northern Jämtland and into southwestern Västerbotten, and NW–SE northwards. Along the eastern Caledonian margin, mineralized veins occupy fractures in the crystalline basement, which were re-activated during broadly E–W-directed extension at c. 544–534 Ma (Billström et al. 2012; Saintilan et al. 2015; 2017; Fig. 3).

In the Lower Allochthon, slices of Palaeoproterozoic crystalline rocks with a lithology similar to the autochthonous basement, occur in all of the discussed thrust systems. On top of these crystalline rocks, sub-Cambrian sedimentary rocks comprise the Cryogenian Risbäck group and the overlying Ediacaran Långmarkberg formation (Figs. 3, 9). These rocks continue from the Risbäck basin established in northern Jämtland and southern Västerbotten in the southwest (Kumpulainen 1982) northwards across the Flakaträsket area and to the Hemfjäll area (Grambow 2001). Towards the north, the Risbäck group ends approximately along the Laisälven River northeast of Laisvall (Greiling et al. 2021) but continues northwestwards in the Tjulån and Gavas windows (Fig. 2, Fig. S11).

The autochthonous lower Cambrian succession

The autochthonous lower Cambrian sedimentary cover between ATC and GOC overlies crystalline basement rocks and is exposed in a narrow strip at the eastern erosional margin beneath the Caledonian nappes (Figs. 1b, 2). It is part of the Dividal Group, comprising, from bottom to top, the Laisberg, Grammajukku, and Alum shale formations (Willdén 1980; Thelander 1982; Nielsen and Schovsbo 2011; Cederström et al. 2022; Figs. 1b, 2, 9, SI Table S1). In the north of the area, around Vietas, the autochthonous cover is restricted to the Grammajukku formation (Thelander 1982; Björklund 1989) and increases in stratigraphic range and thickness southwards until the Laisvall area (c. 100 m). There, the underlying Laisberg formation comprises six members (Willdén 1980), which alternate between quartz arenites, siltstones, and mudstones. Mudstones and siltstones with subordinate fine-grained quartz arenites and occasional carbonate layers and phosphorite fragments dominate the Grammajukku formation. Black, bituminous mudstones characterise the Alum shale formation with occasional grey siltstone layers and subordinate bituminous limestones. The age intervals of the Grammajukku and Alum shale formations are constrained biostratigraphically as late early Cambrian and mid- to late Cambrian, respectively (Moczydłowska et al. 2001; Cederström et al. 2022; Nielsen and Schovsbo 2011, 2015; Fig. 9).

From Laisvall southwards for c. 50 km, exposures of the Laisberg formation are absent (Eliasson et al. 2003; Bergman and Kathol 2018). Further south, they occur intermittently for about 20 km from Lake Storjuktan to the southern side of Lake Storuman (SI Fig. S3). There, quartz arenites, siltstones, and subordinate conglomerates of the Laisberg formation rest on the crystalline basement. Close to the basement surface, bedding in the Laisberg formation dips away from local highs. However, a few decimetres above the basement-cover contact, beds are subhorizontal (SI Fig. S2). At Jipmokberget, conglomeratic beds of one to several metres of thickness form the basal successions (SI Fig. S5). Elsewhere, 0.5 to 2 m-thick beds of coarse-grained quartz arenites with subordinate fine-grained quartz arenites and siltstones represent the basal beds. Clasts consist mostly of quartz or quartzite and subordinate feldspar and fragments of crystalline rocks.

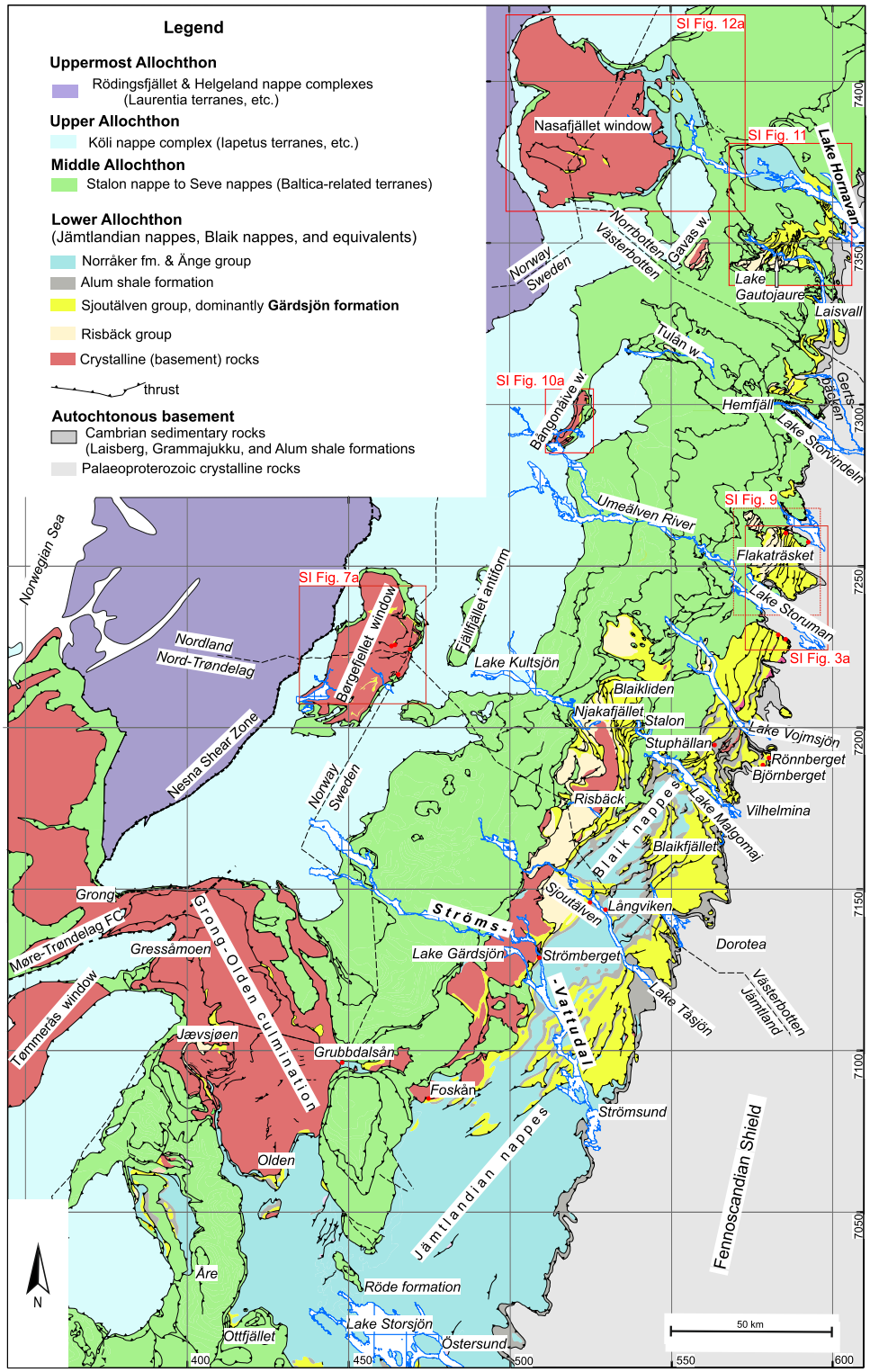

Fig. 2 Map of the contiguous Jämtlandian nappes and Blaik nappes of the Lower Allochthon and their regional context, with locations mentioned in the text and of detailed maps (SI Figs. 3a, 7a, 9–12). Modified from Bergman et al. (2012) and Solli and Nordgulen (2008); FC: Fault Complex

Generally, grains are well rounded with occasional angular grains. In places, isolated clasts of up to 2 cm in diameter occur, which are composed of fine-grained quartz arenite or siltstone. Most layers show quartz cement. Occasionally, carbonate cement led to a differential weathering of, for example, cross-bed laminae or irregular patches where grains stick out. Primary sedimentary structures include planar cross-bedding, current ripples of cm- to dm-scale, and, rarely, wave ripples (SI Fig. S4). Orientations of lee-side laminae of cross-bedding and crests of current ripples

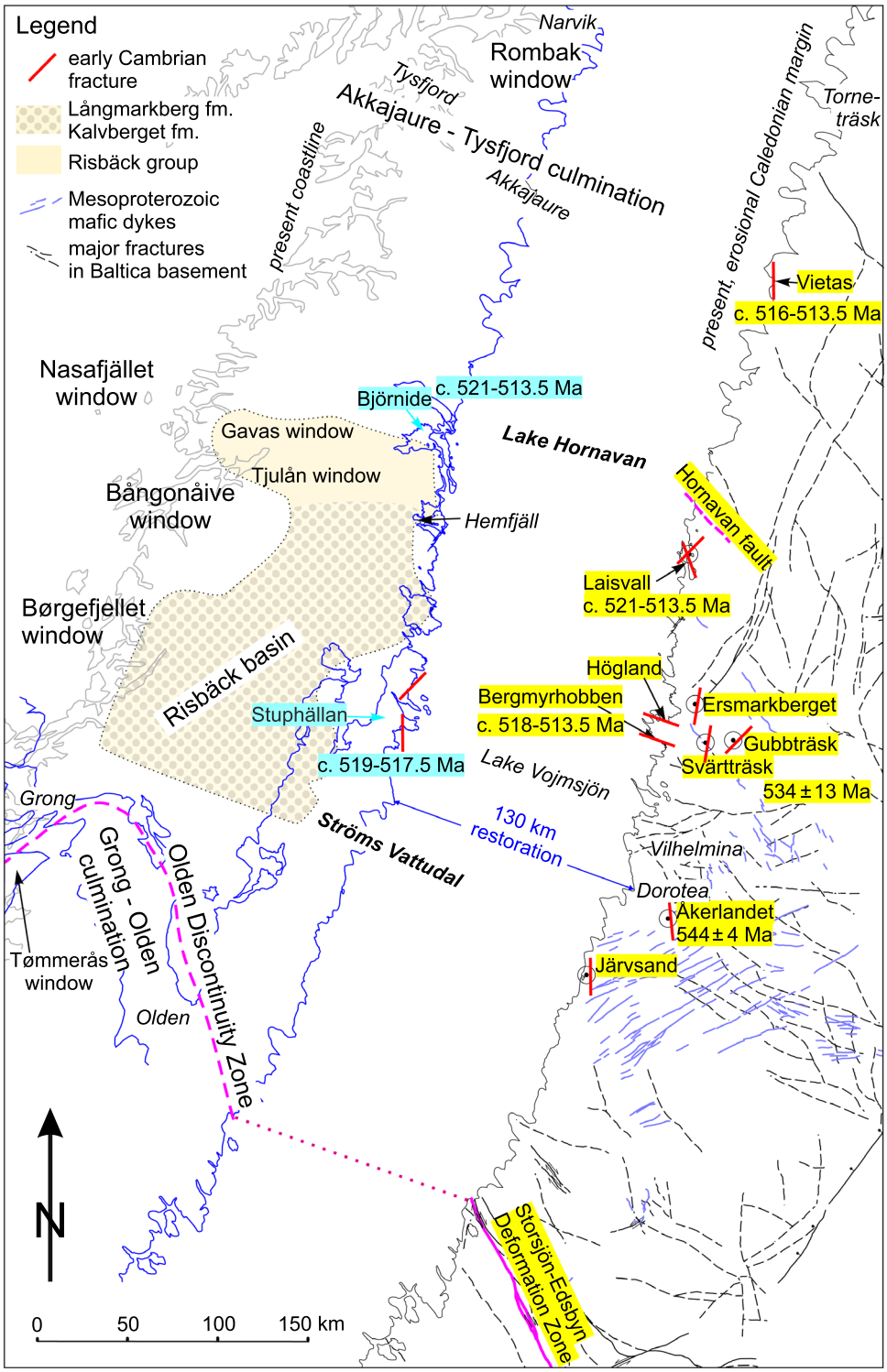

Fig. 3 Early Cambrian fractures and their approximate ages in the autochthonous Baltica basement (yellow label), and the Lower Allochthon (restored, blue label) together with older structural elements, compiled from Bergman and Sjöström (1994), Bergman et al. (2012), Billström et al. (2012), Saintilan et al. (2015; 2017), and this study. See text for details. Windows to the west of the Risbäck basin shown schematically; present coastline in grey. See Fig. 1a for location

indicate a general current direction from east towards west (SI Fig. S3). A thin mudstone veneer covers some of the ripple marks, exposed at the floor of an E–W-oriented channel at Bergmyrhobben. Such a deposit may indicate a transient stage of low energy, perhaps due to changing tides. This is consistent with the position in a tidal (?) channel.

The Laisberg formation reaches more than 12 m of thickness to the west and south of Lake Storuman, but decreases to zero both southwards and northwards, for example at

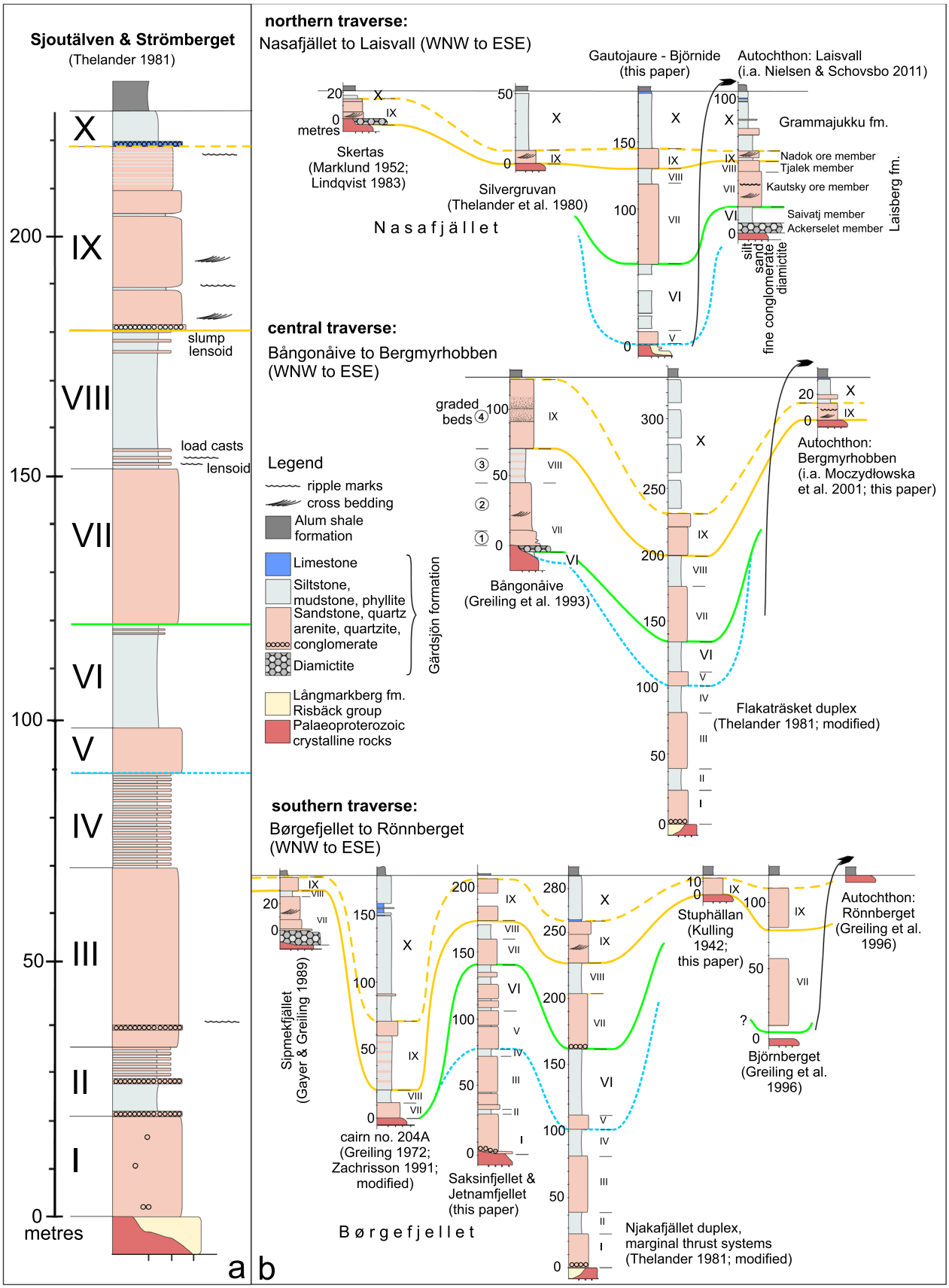
Sjoutälven & Strömberget
(Thelander 1981)
X
IX
slump lensoid
VIII
load casts
lensoid
VII
VI
V
IV
III
II
I
200
150
100
50
0
metres
a
northern traverse:
Nasafjället to Laisvall (WNW to ESE)
Gautojaure - Björnide
(this paper)
Autochthon: Laisvall
(i.a. Nielsen & Schovsbo 2011)
Skertas
(Marklund 1952;
Lindqvist 1983)
Silvergruvan
(Thelander et al. 1980)
Nasafjället
Grammajukku fm.
Nadok ore member
Tjalek member
Kautsky ore member
Saivatj member
Ackerselet member
Laisberg fm.
silt
sand
fine conglomerate
diamictite
central traverse:
Bångonåive to Bergmyrhobben
(WNW to ESE)
graded beds
Bångonåive
(Greiling et al. 1993)
Autochthon:
Bergmyrhobben
(i.a. Moczydłowska
et al. 2001; this paper)
Flakaträsket duplex
(Thelander 1981; modified)
Legend
ripple marks
cross bedding
Alum shale formation
Limestone
Siltstone, mudstone, phyllite
Sandstone, quartz arenite, quartzite, conglomerate
Diamictite
Gärdsjön formation
Långmarkberg fm.
Risbäck group
Palaeoproterozoic crystalline rocks
southern traverse:
Børgefjellet to Rönnberget
(WNW to ESE)
Sipmekfjället
(Gayer & Greiling 1989)
cairn no. 204A
(Greiling 1972;
Zachrisson 1991;
modified)
Saksinfjellet &
Jetnamfjellet
(this paper)
Stuphällan
(Kulling
1942;
this paper)
Autochthon:
Rönnberget
(Greiling et al.
1996)
Björnberget
(Greiling et al.
1996)
Børgefjellet
Njakafjället duplex,
marginal thrust systems
(Thelander 1981; modified)
b

◂**Fig. 4** Lithostratigraphy of the Gärdsjön formation (Gf). **a** Type section with units Gf I to X, compiled from Sjoutälven and Strömberget (Thelander, in Kumpulainen et al. 1981; Gee et al. 1990). **b** Stratigraphic columns of the Gf and its equivalents across the studied area, arranged in three traverses as in the text and Figs. 1b, 6, 7, correlated with Gf I–X at the type section. Correlation lines connect important horizons, also in Figs. 7, 9

Kyrkberget (SI Fig. S3). It reappears at Högland, with a maximum thickness of c. 20 m (Kulling 1942; Greiling et al. 1999) and continues northeast wards to the hill Lillblaiken (Eliasson et al. 2001; 2003). Around Jipmokberget, the thickness of the Laisberg formation of more than 13 m decreases to zero northwards and southwards (Eliasson et al. 2003). SI Fig. S4 and S5 show details of alternating quartz arenites with ripples, planar cross-bedding, and shales, which include trace fossils. South of Bergmyrhobben, and for at least 80 km further towards the south, in the Vojmsjön and Malgomaj areas, the Laisberg formation is absent, save for minor sandstone beds, and the Grammajukku formation rests on basement rocks. To the north and west of Vilhelmina, also the Grammajukku formation is missing, so that the Alum shale formation rests directly on the basement (Bierlein and Greiling 1993; Greiling et al. 1996; 1999; Björk et al. 1996; Fig. 4b: Rönnberget). Further south, the Långviken drill hole (Fig. 2) exposes c. 10 m of quartzite, resting on the crystalline basement (Gee et al. 1978). Such a thin cover continues towards south, across the GOC and to Vassbo (e.g. Nielsen and Schovsbo 2011; Saintilan et al. 2015).

The lower Cambrian successions in the Lower Allochthon: Gärdsjön formation and equivalents

The Gärdsjön formation (in the following abbreviated as Gf) represents the lower Cambrian succession of the Jämtland supergroup (Gee and Stephens 2020; SI Fig. S1, Table S2) and builds up major parts of the Lower Allochthon thrust systems. It comprises ten units, here with the notifications Gf I to Gf X, from bottom to top, used also for correlatives across the present area. The first part gives an overview of the Gf based on the type sections in Ströms Vattudal (Thelander in Kumpulainen et al. 1981; Gee et al. 1990) and our data. The three following parts show regional variations, grouped in traverses oriented broadly from ESE to WNW and normal to the general Caledonian strike direction (see Figs. 1b, 6, 7, SI Table S2).

The Gärdsjön formation, lithology, and constituting sub-units

A > 300 m-thick succession of the Gf is distributed from north of the GOC, around the Strömberget-Sjoutälven-type locations (Gee et al. 1990), across the Njakafjället duplex up to and including the Flakaträsket duplex in the north (Fig. 2). Successions of reduced thickness occur towards the south and towards the eastern Caledonian margin (Gee et al. 1978), northeast wards along this margin, at Vilhelmina (Greiling et al. 1996, 1999), at Hemfjäll (Greiling and Kathol 2021b), and in the Gautojaure–Björnide–Hornavan thrust systems (Lilljequist 1973; Greiling and Kathol 2021a; Greiling et al. 2021). Towards the northwest, in the Børgefjellet, Bångonåive, and Nasafjället windows, successions are thinning as well. Figure 4a shows the Gf type column with its ten units of alternating quartz arenites and siltstones–shales. Lithologically, the quartz arenites with well-rounded quartz grains and a cement of quartz and occasional carbonate are similar to those in the Laisberg formation. Bedding is regular with centimetre- to a few decimetre-thick layers (SI Fig. S6). Conglomeratic beds occur in Gf I to III with clasts composed mainly of quartz and subordinate feldspar, quartzite, and crystalline rocks. Conglomerates of Gf X contain mainly phosphorite fragments in a carbonate matrix. Most of the Gf siltstones and shales with subordinate mudstones (Gf II, IV, VI, and VIII) are dominated by fine-grained quartz, which is often recrystallized. Clay minerals are relatively rare (Greiling 1985; Warr et al. 1996). All these siltstone-shale layers contain centimetre- to decimetre-thick quartz arenite interlayers. Often, millimetre thick, fine-grained quartz arenite layers alternate with finely laminated siltstone or shale. Gf VI is distinct by red coloured interlayers in green siltstones and shales. Red-coloured interlayers in Gf VI are missing from the northeastern part of the Flakaträsket duplex and towards the north, including the Gautojaure and Laisvall areas, but reappear in the Torneträsk area (Fig. 6a). Sedimentary structures comprise ripples (Gf III, VIII, IX), cross-bedding (Gf VII, IX, SI Fig. S6a, b,8c), lensoid layers, slump structures, load casts (Gf VIII), and graded bedding (Gf IX). Directional data are lacking, due to Caledonian overprint and unfavourable outcrop conditions (mostly 2D). Close to the floor and roof thrusts of horses, quartz arenites are recrystallized to quartzites containing abundant quartz veins, siltstones strongly sheared. Such recrystallization is often pervasive in the western areas, particularly in the tectonic windows. Because of their economic importance as host rocks to base metal mineralizations and as construction materials, several authors analysed the composition of the quartzites (Kulling 1942; Stålhös 1958; Du Rietz 1960; Hansson 1977; Willdén 1980). The quartz content is between 90 and 100%, with minor amounts of feldspar and rare clay minerals, locally with subordinate accessories such as fluorite or galena.

Southern traverse: eastern, marginal thrust systems to Børgefjellet window

The southern traverse comprises a zone from the Caledonian margin around Rönnberget in the east and, successively

towards west, the Njakafjället duplex and the Børgefjellet window (Figs. 1b, 2).

Eastern, marginal thrust systems and Njakafjället duplex Published geological maps (Greiling and Zachrisson 1999; Greiling et al. 1996; 1999; Zachrisson 1997; Zachrisson and Greiling 1993; 1996) document the distribution of the Gf. Close to the eastern, erosional margin, the succession is distinctly thinner and, in places (e.g., between Stuphällan and Björnberget, Fig. 2), disappears completely. The Björnberget hill is built up of a quartzite succession, representing the easternmost horse of the Lower Allochthon. From the floor thrust to the overlying Alum shale formation, the succession is somewhat more than 100 m thick. The quartzites with regular, c. decimetre-thick beds represent Gf VII and IX (Fig. 4b). The Stuphällan section (Kulling 1942) comprises c. 12 m of quartzite. It overlies crystalline basement rocks and is covered by the Alum shale formation. The coarse-grained, thickly bedded quartzite corresponds to Gf IX. From Stuphällan westwards, across the Njakafjället duplex (Gayer and Greiling 1989) the Gf is broadly homogeneous and comparable with the type section. The siltstone–mudstone of Gf VI has a thickness of 42–87 m (Zachrisson and Greiling 1993; Greiling and Zachrisson 1999; our data), about twice that at the type location. Its top shows an erosional channel filled with conglomeratic quartz arenite of the overlying Gf VII, composed of well-rounded quartz and subordinate feldspar clasts (SI Fig. S6d–f). In general, quartz arenite beds are of dm-scale with cm- to mm-size layering with various grain sizes, and cm-thick finer-grained interlayers, mostly siltstones (SI Fig. S6a–c). At the top, Gf X is at least 30 to 40 m thick, as interpreted from the Stalon tunnel section (Strand and Kulling 1972). Its basal part contains two c. 40 cm-thick layers of impure limestone, which, in places, is fossiliferous (Kulling 1955).

Børgefjellet window The basement-cover thrust units, as interpreted from the existing detailed maps (Foslie and Strand 1956; Gustavson 1973; Greiling 1988; Zachrisson 1991; SI Fig. 7a) and our data, comprise at least four major horses, two of which (nos. 2, 4) are relevant here. Horse 2 displays relatively complete cover successions, at the NW slope of Mount Sipmekfjället and southeast of border cairn 204A. At the base of the Sipmekfjället section, diamictites, up to 10 m thick, non-conformably overlie gneisses of the Palaeoproterozoic basement (Fig. 4b, SI Fig. S8g, h, Table S2; Greiling 1972). Fragments comprise quartzites, vein quartz, and rare crystalline rocks. They are mostly angular and up to 20 cm in diameter. Overlying the diamictite is a 10- to 20-cm-thick, polymictic conglomerate, with sharp boundaries at both the bottom and the top. It is partly matrix-supported, partly clast-supported. Clasts are of centimetre scale and composed of granite, feldspar and quartz grains, quartzite, greenish phyllite, and rusty weathered rocks, which contain Fe- and Cu-sulphides. The overlying coarse-sandy quartzite succession, composed of whitish–bluish quartz grains and rare white feldspar grains, reaches c. 10 m of thickness. Trough cross-bedding occurs in decimetre-thick layers. The grain size within the cross-bed laminae decreases from the base to the top. This basal succession correlates with Gf VII. The overlying alternating fine sand- and siltstone layers (Gf VIII) are c. 5 m thick and followed by c. 5 m of grey quartzites (Gf IX). At the top, rusty weathered, distinctly radioactive, dark grey shales overlie the quartzites and represent the Alum shale formation (Greiling 1981). About 9 km towards NNE, southeast of border cairn 204A, a c. 175 m-thick section of alternating quartzites and predominantly shales or quartzphyllites underlies graphitic phyllites of the Alum shale formation (Greiling 1972; Zachrisson 1991; Fig. 4b). The lower part with a basal quartzite, overlain by quartz phyllites and a second quartzite member, is comparable with the Sipmekfjället sequence. Overlying quartz phyllites are c. 100 m thick and represent Gf X. In their uppermost part, a conspicuous, c. 8 m-thick succession with calcareous phyllites and quartzites, and a layer with carbonate-bearing fragments in a calcareous–phyllitic matrix is exposed.

In horse 4, a c. 230 m-thick cover succession, capped by sheared alum shale, is evident from the geological map (Greiling 1988). The lower part of this succession is well exposed at the north slope of Jetnamfjellet and the upper part southwest of Saksinfjellet. The column on Fig. 4b is a composite of the two parts, connected by the quartzites of Gf V. At Jetnamfjellet, the Gf quartzites fill up a relief in the basement rocks in the order of a few metres (SI Fig. S2b). At the base, c. 50 cm-thick conglomeratic quartzite non-conformably overlies Palaeoproterozoic, mica-rich gneisses with dykes of the Børgefjellet granite. Conglomerate clasts are composed of quartzite and, rarely, feldspar. Most of the quartzite clasts are flattened, due to deformation, but feldspar-dominated clasts retain a round shape. The overlying succession is rather uniform with glassy quartzites, foliated at a millimetre to centimetre-scale, which are alternating with more mica-rich, brownish weathering phyllitic quartzites.

Central traverse: Flakträsket duplex to Bångonåive window

The central traverse covers the Flakaträsket duplex in the east and, towards west, the Bångonåive antiformal stack (Fig. 1b, 2).

Flakaträsket duplex The Flakaträsket duplex, extending along strike for c. 20 km and more than 30 km across strike with at least 21 horses (Febbroni 1997; Eliasson et al. 2001; 2003; Greiling et al. 1999; Greiling and Kathol 2021d;

Fig. 2, SI Fig. S9), rests on autochthonous rocks between Lakes Storuman and Storjuktan. Except for the four westernmost horses, the complete section of Gf I to X is preserved, including the northernmost occurrences of the red-green shales of Gf VI (Greiling and Kathol 2021c). The thickness is generally around 300 m. With 70 to 170 m (100 m on Fig. 4b), Gf X is distinctly thicker than at the type location.

Bångonåive window The Bångonåive window exposes at least four basement-cover horses (Greiling et al. 1993; Stephens 2001; SI Fig. S10). Stephens (1977) named the c. 150 m-thick cover succession with quartzites and pelites as Oltokken formation, composed of parts 1 to 4. Overlying radioactive shales of the Alum shale formation suggest it as an equivalent of the Gf and the four parts correspond to Gf VII to IX (Fig. 4b). On top of crystalline basement rocks, the basal beds in horses 1, 2 comprise coarse-grained diamictite and arkosic micro-breccia or fine conglomerate, followed by a succession of whitish quartzites with occasional cross-bedding (Gf VII). In horse 3, a few metres of greenish phyllites underlie the Gf VII diamictites and represent Gf VI. An alternation of fine-grained quartzites and greenish-grey siltstones/phyllites, overlain by grey-to-dark grey quartzites, represent Gf VIII and IX, respectively. In places, the latter quartzites show graded beds at a decimetre scale.

Northern traverse: eastern, marginal thrust systems to Nasafjället window

The traverse covers the zone from Hemfjäll to Hornavan at the eastern Caledonian margin (Figs. 1b, 2). The Hemfjäll area shows a duplex structure (Bergman and Kathol 2018; Eliasson et al. 2003; Greiling and Kathol 2021b). There, the Gf comprises units V to X and is overlain by the Alum shale formation. The thickness is somewhat more than a hundred metres. Further west, the Gf is missing in the Tjulån and Gavasjaure windows (Greiling and Kathol 2021a). Towards the north, however, the Gf is extensively exposed in the Gautojaure-Björnide area and, towards the northwest, in the Nasafjället window.

Gautojaure–Björnide–Hornavan thrust systems Published geological maps (Bergman and Kathol 2018; Greiling and Kathol 2021b; Greiling et al. 2021; Lilljequist 1973) document the Gf. South of Lake Gautojaure, the Gf overlies coarse, poorly sorted conglomerates and arkoses of the Risbäck group, which rest on felsic, crystalline basement rocks (SI Fig. S11). The Risbäck group disappears successively towards north and, north of Lake Gautojaure the Gf directly overlies the crystalline basement. Around the eastern end of Lake Gautojaure and at Björnide, Gf VII to X and the overlying Alum shale formation are well documented at the surface and in drill-hole sections (Greiling and Kathol 2021a; Sveriges geologiska undersökning 2020). A c. 50 m thick succession of greenish-grey shales and siltstones, often alternating with centimetre-thick fine-grained quartzites, underlies Gf VII quartzites. Though lacking the characteristic red and green colours as observed further south, it is equivalent with Gf VI (Saivatj member, Willdén 1980). In the adjacent thrust units, an underlying quartz arenite at the base of the Gf represents Gf V. The thickness of the Gf reaches up to c. 200 m and decreases northwards (SI Fig. S11). In some of the Björnide drill-hole sections (interpreted from original logs by F. Kautsky 1948 (unpulished report); Sveriges geologiska undersökning 2020), Gf X attains a thicknesses of 24 m to > 84 m (40 m in Fig. 4b), which is considerably thicker than the c. 20 m observed at the surface. However, in other drill holes, the Alum shale formation directly overlies basement granite. Recent mapping around Lake Gautojaure (Bergman and Kathol 2018; Greiling and Kathol 2021b; our data) showed that the rocks, which were earlier mapped as greywackes and supposed to be of Ordovician age (e.g., Lilljequist 1973), correspond to the finer-grained members of Gf VII to X. They show a primary contact towards the overlying Alum shale formation, which forms the top of the respective thrust units. To the west of Lake Hornavan, however, overlying fossiliferous greywackes of the Ordovician Norråker formation are preserved (Thelander 2009; Bergman and Kathol 2018; SI Fig. S11).

Nasafjället window The Nasafjället window exposes at least eight thrust units (horses 1–8), as interpreted from the maps of Gjelle (1988), Thelander et al. (1980), Bergman et al. (2012), Silvennoinen et al. (1987), and the archives of the Geological Survey of Sweden (SI Fig. S12). In the eastern, Swedish part of the Nasafjället Window, Thelander et al. (1980) summarised the cover successions as Mierkenis Group. At the south-eastern margin of the window, around Skertasåive or Skuortatjåkkå, a succession of quartzites, quartz arenites with clay pebbles, and grey shales together with overlying black, graphitic shale, make up the Skertas formation (Marklund 1952; SI Table S2). It compares well with the cover succession at Laisvall (Thelander et al. 1980), and quartzites and shales with Gf IX—X (Fig. 4b). The black, graphitic shales represent the Alum shale formation as confirmed by their characteristic radioactivity and trace-element contents (Lindqvist 1988). In the south and the west of the Nasafjället window (horses 1–3), the alum shales are the highest stratigraphic level preserved (e.g. Marklund 1952; Thelander et al. 1980; Lindqvist 1988). In the Storselet area, a "lower unit of quartzites and occasional graphitic phyllite with abundant grey phyllites above" (Thelander et al. 1980) overlies the basement rocks. Quartzites preserve traces of cross-bedding. Directional data are missing. Since the quartzites directly underlie the graphitic phyllite of the Alum shale formation, they are correlated

here with Gf IX (in contrast to Gf VII of Thelander et al. 1980). The grey, sometimes calcareous phyllites above correlate with lower to middle Ordovician greywackes of the Norråker formation at Hornavan (Silvennoinen et al. 1987; Bergman et al. 2012).

Because of the strong deformation, primary thicknesses of the cover successions in the Nasafjället Window can only be inferred from relatively little deformed sections at its southern margin (Marklund 1952; Lindqvist 1988) and the Silvergruvan and Storselet areas (Thelander et al. 1980). Accordingly, the Skertas formation or Gf IX–X attain a thickness of 20 m or less. At Nasafjället, the Silvergruvan section shows several tens of metres of phyllites (Gf X), overlying the quartzites and capped by the Alum shale formation.

Restoration of Caledonian thrusts and basin geometry

To constrain the geometry of the original distribution of Gf deposits, Caledonian shortening is restored by balancing structural sections parallel with the general WNW–ESE transport direction of the Lower Allochthon, according to thrust-related lineation data, branch lines of nappes and horses (e.g. Hossack and Cooper 1986; Gayer and Greiling 1989; Greiling et al. 1993, 2018; Rice and Anderson 2016). The dip of the regional floor thrust towards WNW with an angle of c. 2° can be assessed at the erosional Caledonian margin from outcrop patterns along major valleys (e.g. Greiling et al. 1996) and from extensive exploratory drilling in the Ormsjön–Tåsjön area (Du Rietz 1960; Gee et al. 1978) and around the Laisvall mine (Lilljequist 1973). Further west, the depth of the regional floor thrust at the Børgefjellet window is estimated from the depth of the adjacent synforms (Greiling et al. 1998), at the Bångonåive window from geophysical data (Dohme & Greiling 1981), and consistent with the 2° dip. This value is on the conservative side as compared to dip angles of up to 5° in the Östersund region (Gee & Stephens 2020). The observed minimum thrust distance from the outcrop pattern of the erosional margin and from drill holes is c. 40 km (Du Rietz 1960; Gee et al. 1978; Lilljequist 1973). Based on general wedge geometry (e.g. Davis et al. 1983), Hossack and Cooper (1986) and Rice and Anderson (2016) suggested additional thrust distances of more than 100 km to compensate for the eroded parts of the syn-orogenic wedge tip. Metamorphic data of the autochthonous succession at the eastern margin imply an overburden corresponding to an orogenic wedge extending c. 130 km towards the foreland as modelled by Warr et al. (1996). In want of more precise data, maps, and sections Figs. 6 and 7 use the value of 130 km for a first step of restoration.

The Njakafjället duplex, where the roof thrust is sufficiently well preserved, reveals a shortening in the order of 50% (46–54%, Gayer and Greiling 1989; Grimmer and Greiling 2004). Such a value is valid also for the Lower Allochthon at a regional scale (e.g. Morley 1986; Greiling and Garfunkel 2007; Rice and Anderson 2016). Where erosion removed the upper parts of the marginal thrust systems, restoration relies on this general value. In the section across the Hornavan area, shortening in the dominant Norråker formation with greywackes and shales, largely by cleavage formation, is taken as no less than 50% (e.g. Greiling and Garfunkel 2007). Figure 5 summarises the results and gives the amount of shortening. Numerical values for the restored lengths of sections may have errors of > 10%. However, the relative position of the lower Cambrian units (Fig. 6) is well constrained. The second step of restoration of the marginal thrust units moves the overlying nappes as a passive roof towards west. In the Gautojaure and Hornavan sections, this leads to an overlap of the restored Gf over the Gf in the Nasafjället window towards the west (blue bracket in Fig. 6a). Therefore, this window has to be restored towards the west until it is no longer covered. Since all of the windows are covered by a contiguous passive roof of overlying nappes, also the Bångonåive and Børgefjellet windows are moved accordingly. This is justified by the absence of any traces of differential movement in the nappe transport direction. It may also compensate for local shortening, which cannot be quantified in the Gavas and Tjulån windows and the Fjällfjället antiform (Fig. 2; Greiling et al. 1998). Subsequently, the sections of the windows are restored. At the Nasafjället window, this step leads to another overlap, since the Gf in the Høgtuva window is now covered by the Nasafjället Gf (green bracket in Fig. 6a). Accordingly, the Høgtuva window requires another step of restoration towards west (red contours). To assess the basin geometry, Fig. 6a and b shows a restoration across the area, based on the 2D section-balancing results (Fig. 5).

To the west of the area, late-Caledonian extension or transtension overprinted the Caledonian nappe pile (Dewey and Strachan 2003; Osmundsen et al. 2003). Extension between Nasafjället and Høgtuva is of little significance at the scale of the present study, but towards south, the Nesna Shear Zone (NSZ; Fig. 1b) represents considerable displacement. Therefore, the balanced sections stop at the NSZ west of the Bångonåive and Børgefjellet windows (Fig. 7).

Sedimentary structures and environment

Quartz arenites with conglomerates dominate the early Gf successions I, II, V, whilst siltstones and mudstones of Gf II, IV are of relatively minor thickness. Ripple marks in Gf II reflect shallow water conditions. Siltstones and mudstones of Gf VI represent a transgression–regression cycle with widespread drowning (Thelander 1982; Nielsen and Schovsbo 2011). At Laisvall, Willdén (1980) interpreted Gf VI as

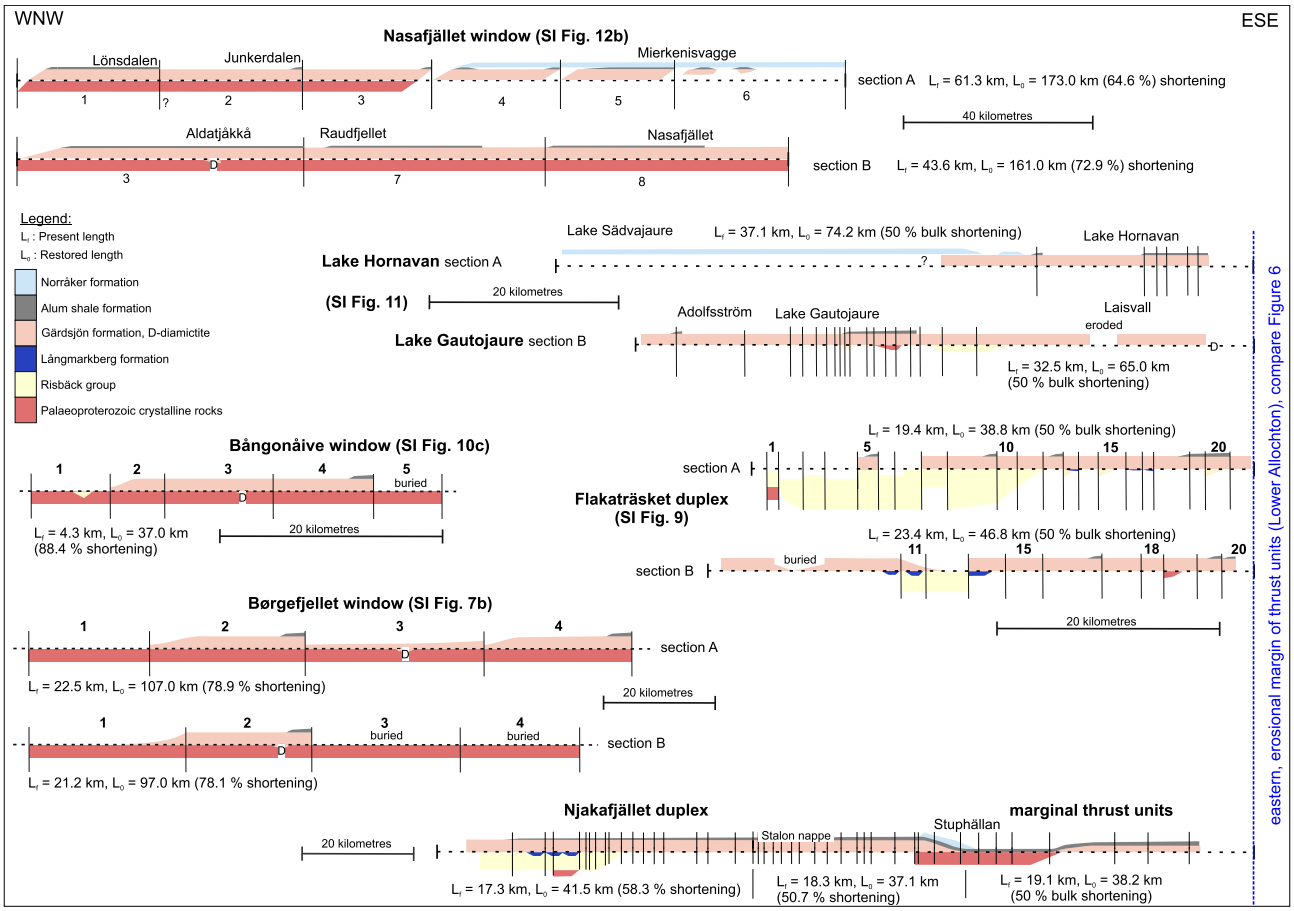

Fig. 5 Restored sections across the studied area showing a pre-Caledonian configuration of the Gärdsjön and equivalent formations. Structural boundaries appear schematically as vertical lines. For the thrust systems extending from the eastern margin a bulk shortening of 50% is restored. The Njakafjället duplex, Børgefjellet, Bångonåive, and Nasafjället sections show the results of line–length balancing along the base of the Gärdsjön formation from the sections of the respective SI Figs. (7b, 10c, 12b). Njakafjället duplex based on Zachrisson and Greiling (1993; 1996) and Greiling et al. (1996). Thicknesses shown schematically

a bay deposit, which indicates proximity to the eastern HVB margin. Overlying basal conglomeratic beds of Gf VII in the Njakafjället area, with mostly quartz and some feldspar clasts (SI Fig. S6d) fill minor channels eroded into Gf VI shales (SI Fig. S6e, f). In the Nasafjället and Børgefjellet areas, competent quartzite beds (Gf VII, IX) show traces of cross-bedding (SI Fig. S6b, 8c; Thelander et al. 1980), indicating shallow water. At the eastern margin at Laisvall, Willdén (1980) documented various examples of near shore environments during deposition of Gf VII and IX, with ripple crests in Gf VII indicating E- and W-directed currents, and NW and NE directions in Gf IX. In the Storuman area, cross-bedded layers and current ripples in Gf IX are generally well preserved (SI Fig. S3a, 4-6). The dips of the foresets towards W (SW to NW) indicate a general current in this direction. Orientations of asymmetric ripples, some of which occur at the floor of a (tidal) channel, are consistent with W-directed currents. Exceptionally, in the north of the Storuman area (Jipmokberget, SI Fig. S4a, 5), foresets and ripples document currents towards NW to NE. Ripple marks at Laisvall (Willdén 1980) and Storuman indicate shallow water conditions. Further west, at Bångonåive, graded beds (Stephens 1977) point to deeper water on the shelf, being probable tempestites. The overlying mudstones and siltstones of Gf X at Laisvall and Storuman show transitions towards sandy deposits in the east, close to the basin margin. Towards the west, Gf X shales are rather uniform, though with variable thicknesses. Limestone layers close to their base suggest initial shallow water conditions, which change upwards to deeper water due to subsidence of the basin floor. At the top, rare limestone lenses and phosphorite fragments (e.g. Greiling and Kathol 2021a) suggest shallowing.

Syn-sedimentary faults and major normal faults

The lower Cambrian successions preserve several faults that were active during sedimentation (Figs. 3, 8, SI Fig. S4b). Around Laisvall, Saintilan et al. (2015) provide a review

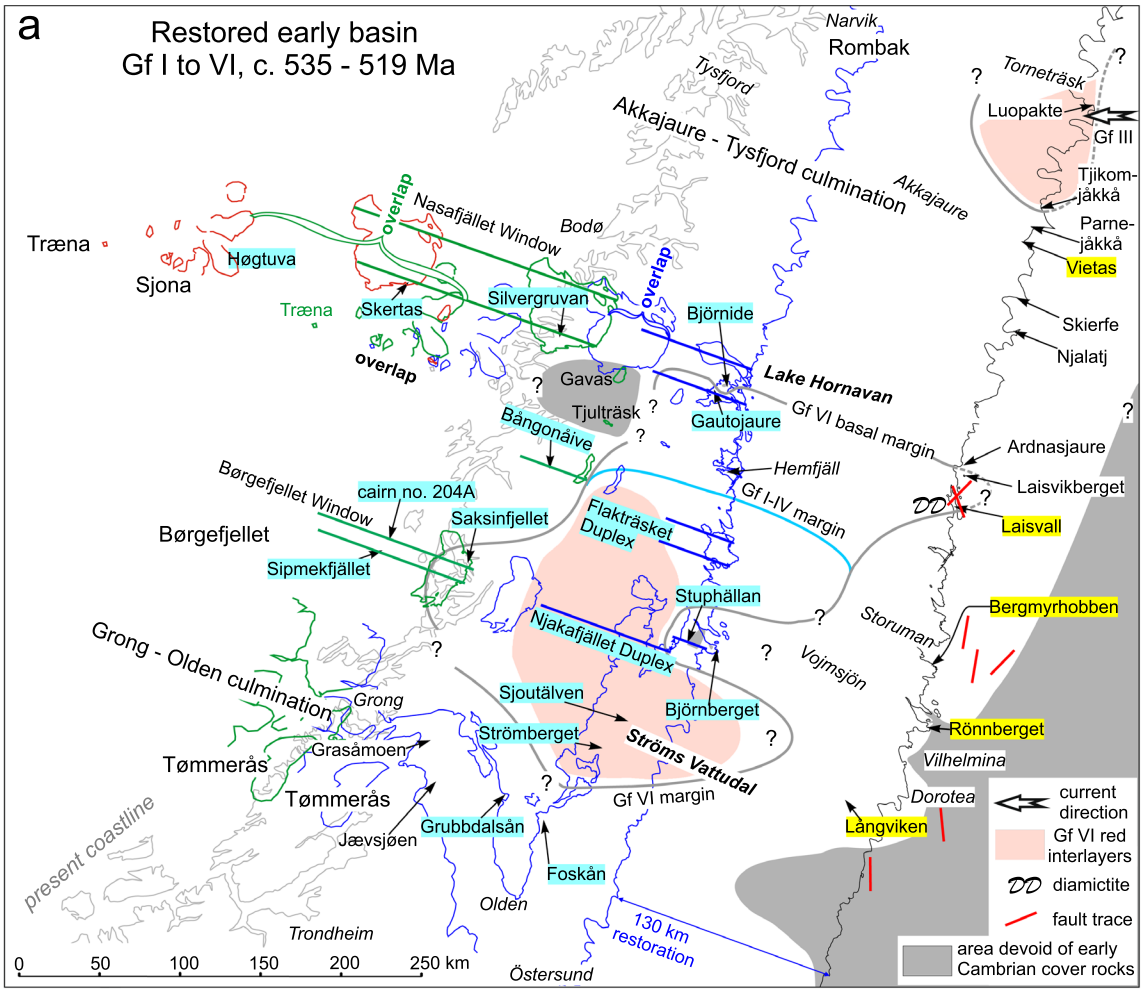

Fig. 6 **a** Section restoration of the study area in map view, based on restored sections of Fig. 5 (lines in WNW, 110°; directions, coloured according to restoration stage). Blue contours represent boundaries restored for 130 km towards WNW. Blue straight lines show locations of balanced sections in marginal thrust systems after restoration of 130 km. Overlap of restored Gf over Nasafjället window (blue bracket) requires restoration to green position, which also includes Bångonåive and Børgefjellet windows. Straight green lines represent restored sections of windows. Restored Gf of Nasafjället window overlaps over Høgtuva area (green bracket) and requires further restoration westwards to red position. Arrow tips show locations of stratigraphic columns of autochthonous successions (yellow labels) and of the restored Lower Allochthon (blue labels) from Fig. 4. Further locations along the eastern margin from Thelander (1982; 1994), in the Grong-Olden area from Gee (1974), Schenk (1975), Walser (1980), and at Høgtuva from Lindqvist (1988). Basin margins dashed where eroded; **b** as **a** for Gf VII–IX, symbols for current directions and diamictites coloured according to age (as basin margins), dotted orange lines show locations of sections in Fig. 5. Basin margins dashed where eroded

on basement fractures, supported by geophysical modelling. Accordingly, a set of NE–SW to N–S and WNW–ESE to NW–SE-trending basement faults are re-activated during deposition of Gf V to X. Towards the north, broadly along Lake Hornavan, the NW–SE trending Hornavan fault (Saintilan et al. 2015; Fig. 3) produced flexures in the Cambrian beds (Kathol et al. 2012). Above a W-dipping normal fault within the Gf VIII quartzite succession, layer thicknesses increase markedly towards the fault (Fig. 8a, Björnberget). At least one layer shows a corresponding upward increase in grain size from sand to conglomerate at its top, implying a syn-sedimentary or growth fault activity. Some beds are kinked without any ruptures, indicating a ductile behaviour and incomplete lithification. The N–S fault strike suggests broadly E–W-directed extension. A similar fault from an adjacent location has an NE-orientation and broadly SE–NW-directed extension. Relatively thick, coarse quartzite beds, overlie the faulted succession of c. dm-thick beds. They represent the base of Gf IX and imply a tectonic activity during the deposition of the underlying Gf VII and VIII. Further to the east, a minor normal fault in Gf IX is exposed over c. 3 m with a trend of ESE-WNW (110°; Luleluoktberget, Fig. 8b, c). It downfaults the northern side with a maximum throw in the order of 5 cm, consistent with the

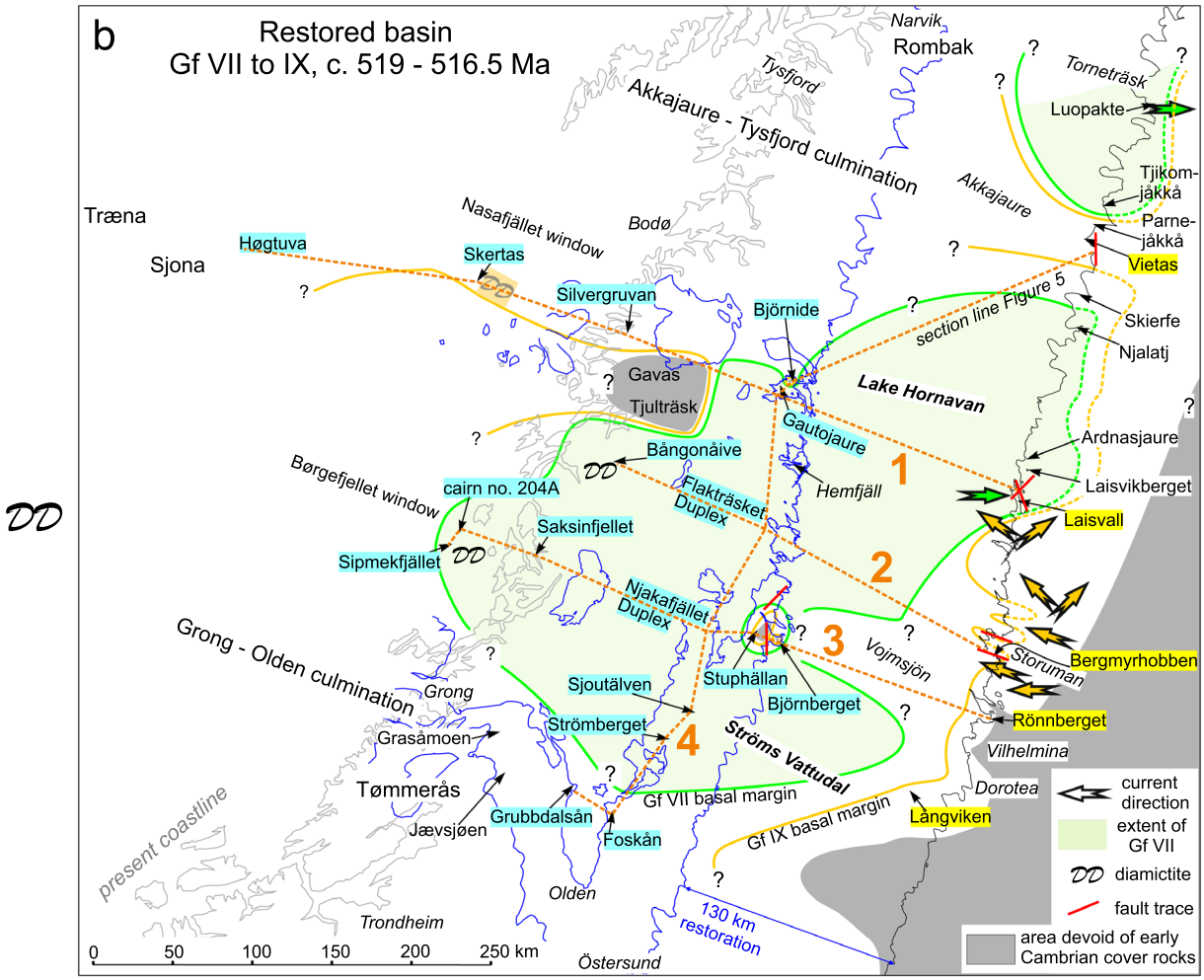

Fig. 6 (continued)

thickening of the quartzites towards north (Greiling et al. 1999; SI Fig. S3b). In places, the fault developed minor splays, which produced a stair-step geometry. Semi-ductile drape folds suggest a deformation prior to complete lithification of the quartz arenite. Similar normal faults occur at the top of Gf IX (SI Fig. S4b). Thickness variations of Gf X across the area (Fig. 4, SI Fig. S3b), at Björnide (Sveriges geologiska undersökning 2020) and Vietas (Hansen 1989), suggest further syn-depositional faulting. In the Storuman area, a set of parallel quartz arenite dykes extends over lengths of more than 20 m (Thelander, in Greiling et al. 1999; our observations) in basement granite close to the basement–cover interface (Fig. 8d, SI Fig. S3). The dykes strike ESE–WNW (110°) with subvertical dips. Dyke thicknesses reach a decimetre or more, and the vertical extension is at least half a metre and continues towards depth. The dykes consist of even-grained quartz and some feldspar grains with a diameter of around 1 mm, comparable with that of the overlying quartz arenites of the Laisberg formation (Gf IX). A c. 5 cm-thick dyke shows a splay or bridge structure of basement rock extending across the dyke (Fig. 8d), which indicates a tectonic origin and NNE–SSW-directed extension.

The observations on outcrop scale fractures complement the interpretation of major normal faults, as inferred on the maps (Fig. 6) and cross sections (Fig. 7). At the eastern margin of the HVB, faults at Laisvall are well documented (Saintilan et al. 2015). To the NW of Laisvall, faults inferred from the Björnide drill cores (Sveriges geologiska undersökning 2020) are related to the northern termination of Gf VI–VIII ("Introduction", 4, Fig. 7, SI Fig. S11). In "Discussion" (Fig. 7), the increase of thickness west of Bergmyrhobben may indicate a normal fault at the eastern basin margin. Minor faults around Lake Storuman mark the northern margin of the WNW–ESE oriented horst-like high area extending from the eastern margin to Stuphällan (Fig. 6b). There, minor normal faults are related to major faults between Stuphällan and Björnberget (Fig. 7, Sect. 3). Further west,

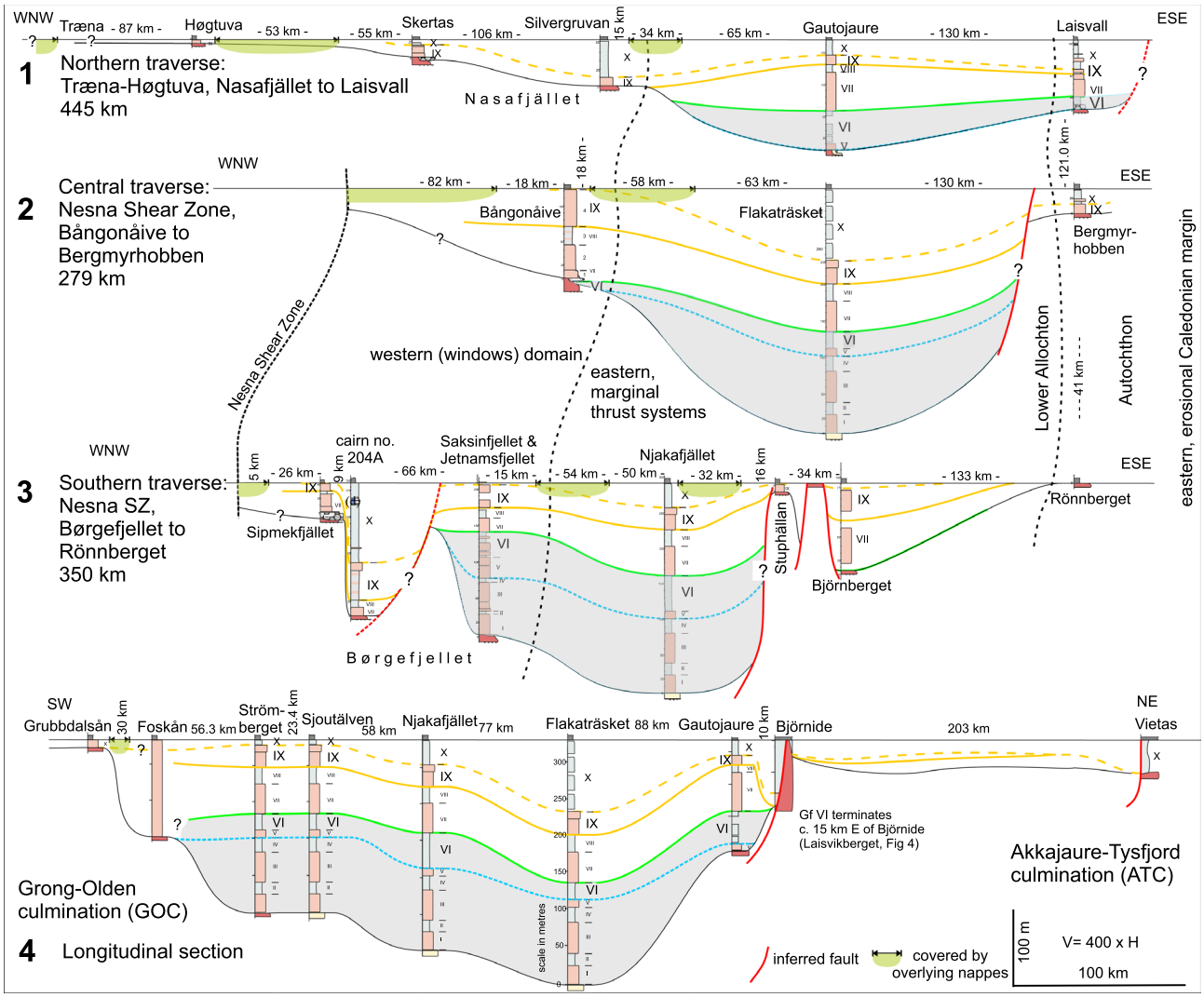

Fig. 7 Schematic sections across the Hornavan–Vattudal basin (HVB), see Figs. 1b, 2 for locations. Columns compiled from Fig. 4 and our data. Grey shading covers the early HVB (Gf I-VI)

variations in thickness between the Børgefjellet locations imply further normal faults.

Biostratigraphy and age data

Figure 9 summarises the available age information on the lower Cambrian strata of the area. The autochthonous succession, reviewed by Moczydłowska et al. (2001), Nielsen and Schovsbo (2011), McLoughlin et al. (2021), and Cederström et al. (2022), is relatively well constrained biostratigraphically. Accordingly, the Grammajukku formation with *Holmia kjerulfi* and *Holmia lapponica* as diagnostic trilobites is of broadly Vergalian–Rausvian age. In the Torneträsk formation of northernmost Sweden, Nielsen and Schovsbo (2011), McLoughlin et al. (2021), and Cederström et al. (2022) confirm Thelander's (1982) correlation of the Upper siltstone member, with the Grammajukku formation. In the underlying succession, the Red and green siltstone member contains *Platysolenites*, and the Lower Siltstone member *Sabellidites* fossils, which indicate Lontovan and Rovnian ages, respectively (Jensen and Grant 1998). For the Lower Allochthon, Nielsen and Schovsbo (2011) summarised stratigraphic data from around the Gf type sections. Underlying beds (Långmarkberg formation) are related to the Marinoan glaciation (Kumpulainen et al. 2021; see, however, cautionary note of Rice 2023) and c. 635 Ma old. There is thus a hiatus of about 100 Ma prior to Gf sedimentation. Following Nielsen and Schovsbo (2011), the base of the Saivatj member or Gf VI, is broadly equivalent with the base of the Dominopolian. At the top of the Gf, Weidner et al. (in Greiling and Kathol 2021a) discovered *Holmia lapponica* in Gf X of the Hemfjäll area, constraining a Vergalian–Rausvian age.

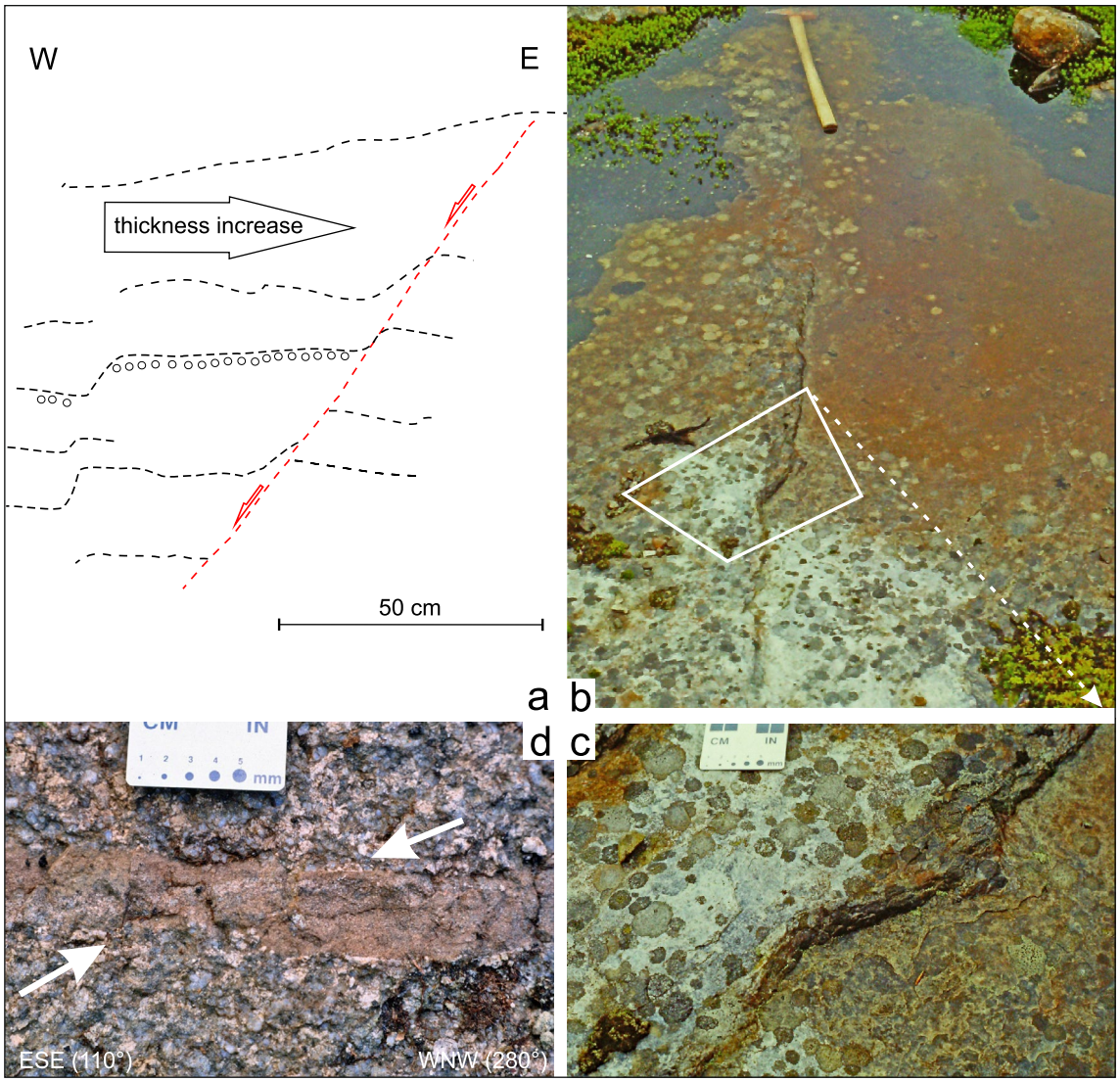

Fig. 8 Examples of extensional structures. **a** Line drawing from field image and sketch of vertical outcrop face showing fault trace (red dashed line with arrows) in quartz arenite (Gf IX; bedding trace: dashed black line), dipping towards WNW (291°), view towards the north. Small open dots mark a conglomeratic horizon at the top of a layer. Note thickness increase in the hanging wall block towards the fault. Björnberget; see Fig. 2 for location. **b** Normal fault and flexure in quartz arenite (Gf IX; to the left of and parallel with hammer handle), view towards WNW. Luleluoktberget, see SI Fig. S3a for location. **c** Detail of **b** marked with a white box, shows part of the fault, branching into minor fractures, causing a step geometry and bending or drag. **d** Detail of quartz arenite dyke in basement granite with a "transfer zone" (arrows) documenting tectonic extension. Högland, see SI Fig. S3a for location

Therefore, this unit correlates with the Grammajukku formation. For a sequence stratigraphic division, preservation of the relevant features in the Gf is insufficient, in particular due to Caledonian deformation and very low- to low-grade metamorphism. However, traces of low stand and drowning events as outlined by Nielsen and Schovsbo (2011) are more easily recognisable in the alternating sandstone and siltstone successions and are related here to the respective lithological changes. Therefore, the combination of biostratigraphic data and sea-level information gives a reliable time frame for most of the Gf successions studied here (Figs. 4, 9). Sea-level events or facies changes control the boundaries of the lithological sub-units and may, therefore, not be strictly synchronous. As a consequence, stratigraphic and absolute ages are only approximate. The base of Gf I is taken as 535 Ma, close to the end of extensional faulting in the basement. The boundary between Gf I and II is taken arbitrarily as the time of a coastal onlap (Fig. 9). Similarly, the Gf IV/V boundary is related to the Hadeborg Drowning. The base of Gf VI (Saivatj member, red and green siltstone member) is at the time of the Brantevik Drowning. Its top corresponds to the Snogebæk lowstand, consistent with terrestrial deposits

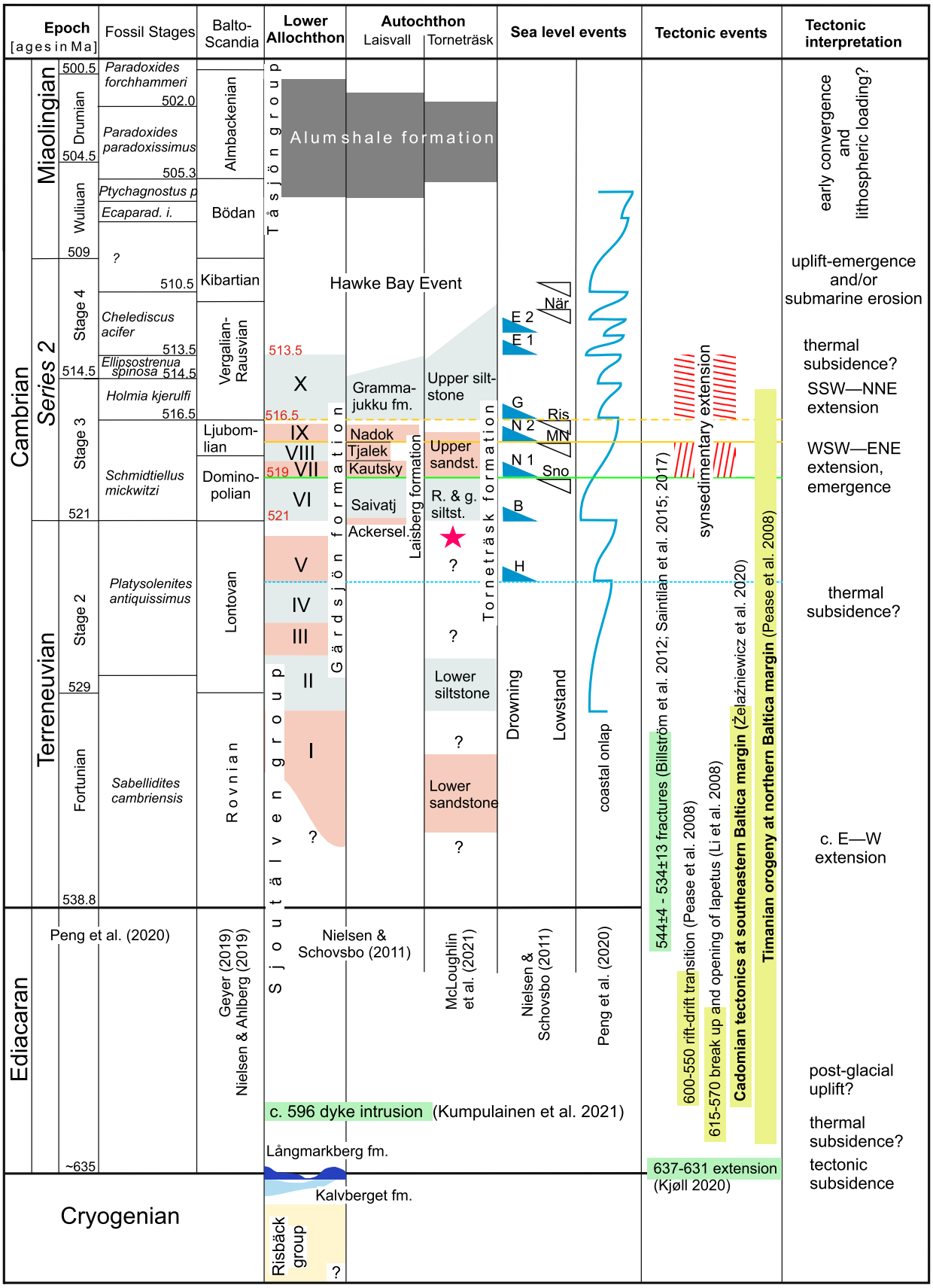
Epoch [ages in Ma]
Fossil Stages
Balto-Scandia
Lower Allochthon
Autochthon
Laisvall
Torneträsk
Sea level events
Tectonic events
Tectonic interpretation
Cambrian
Miaolingian
Series 2
Terreneuvian
Ediacaran
Cryogenian
Drumian
Wuliuan
Stage 4
Stage 3
Stage 2
Fortunian
500.5
502.0
504.5
505.3
509
510.5
513.5
514.5
516.5
519
521
529
538.8
~635
Paradoxides forchhammeri
Paradoxides paradoxissimus
Ptychagnostus p
Ecaparad. i.
?
Cheledicus acifer
Ellipsostrenua spinosa
Holmia kjerulfi
Schmidtiellus mickwitzi
Platysolenites antiquissimus
Sabellidites cambriensis
Almbackenian
Bödan
Kibartian
Vergalian-Rausvian
Ljubom-lian
Domino-polian
Lontovan
Rovnian
Tåsjön group
Alum shale formation
Hawke Bay Event
Gärdsjön formation
Sjoutälven group
X
IX
VIII
VII
VI
V
IV
III
II
I
Gramma-jukku fm.
Nadok
Tjalek
Kautsky
Saivatj
Ackersel.
Laisberg formation
Upper silt-stone
Upper sandst.
R. & g. siltst.
Torneträsk formation
Lower siltstone
Lower sandstone
När
E 2
E 1
G
N 2
N 1
B
H
Ris
MN
Sno
Drowning
Lowstand
coastal onlap
synsedimentary extension
544±4 - 534±13 fractures (Billström et al. 2012; Saintilan et al. 2015; 2017)
600-550 rift-drift transition (Pease et al. 2008)
615-570 break up and opening of Iapetus (Li et al. 2008)
Cadomian tectonics at southeastern Baltica margin (Żelaźniewicz et al. 2020)
Timanian orogeny at northern Baltica margin (Pease et al. 2008)
637-631 extension (Kjøll 2020)
early convergence and lithospheric loading?
uplift-emergence and/or submarine erosion
thermal subsidence?
SSW—NNE extension
WSW—ENE extension, emergence
thermal subsidence?
c. E—W extension
post-glacial uplift?
thermal subsidence?
tectonic subsidence
Peng et al. (2020)
Geyer (2019)
Nielsen & Ahlberg (2019)
Nielsen & Schovsbo (2011)
McLoughlin et al. (2021)
Nielsen & Schovsbo (2011)
Peng et al. (2020)
c. 596 dyke intrusion (Kumpulainen et al. 2021)
Långmarkberg fm.
Kalvberget fm.
Risbäck group
?

◂**Fig. 9** Early Cambrian age and related data. Schematic stratigraphic columns of early Cambrian successions in the Lower Allochthon, at Laisvall, and Torneträsk (colours and correlation lines as in Figs. 4, 6 and 7). Blue triangles mark "drowning", open triangles "lowstand" (Nielsen and Schovsbo 2011; see Fig. 10 for abbreviations). R & g: Red and green; star marks stratigraphic position of Vakkejokk breccia at Torneträsk. For further references see text

at the base of the overlying Gf VII. The Gislöv Drowning marks the base of Gf X (Grammajukku formation, Upper siltstone member). The top of Gf X is at about the time of the Evjevika 1 and/or 2 Drowning events. The Gf is followed by a hiatus, related with the Hawke Bay event. If compared with coastal onlap and third-order sequences from other parts of the globe (Peng et al. 2020), the base of both Gf VI and Gf X may relate to an onlap of global significance.

Early Cambrian subsidence

Sediment thicknesses (Fig. 4) and age information (Fig. 9) indicate the subsidence history of the studied part of the Baltica passive margin (Fig. 10). Whilst compaction in the quartz arenites and quartzites is insignificant (e.g., Greiling et al. 1999a), siltstones–mudstones and phyllites show considerable compaction. Therefore, thickness values of the two major siltstone–mudstones, Gf VI and X, are doubled, representing a thickness prior to 50% compaction, which is within the range of general compaction values (e.g. Mattern et al. 2018).

The curves from the Gf type area (Sjoutälven–Strömberget) and from the Njakafjället, Børgefjellet–Jetnamfjellet, and Flakaträsket areas originate at 535 Ma with Gf I–IV, prior to Hadeborg Drowning (Nielsen and Schovsbo 2011; Fig. 9). Northwards, in the Bångonåive, Gautojaure, and Laisvall areas, the onset of sedimentation occurred with Gf V and VI, until c. 521 Ma. Overlying diamictites or basal breccias are related to the Snogebæk Lowstand. This low stand may have led to complete emergence and ended the early stage of the HVB. Norretorp 1 Drowning (c. 521 Ma) initiated Gf VII and extended the sedimentation area in the Børgefjellet (cairn 204A, Sipmekfjället) and into the Nasafjället (Skertas) areas. Subsequently, the Norretorp 2 Drowning at c. 517.5 Ma (Gf IX) covered additional areas from Bergmyrhobben in the east to Nasafjället–Silvergruvan in the west. Finally, an increase of the apparent subsidence rate in parts of the area during Gf X relates to Gislöv Drowning at c. 516.5 Ma. A substantial hiatus follows the top of Gf X at c. 513.5 Ma, until the deposition of the Alum shale formation from c. 506 Ma. Early subsidence related to Gf I–VI is followed by emergence and erosion, which may have removed a part of the succession. Accordingly, the subsidence rate of c. 140–230 m in c. 16 Ma (~9–14 m*Ma^{-1}) in the HVB centre is probably lower than the original value. A second stage of subsidence comprises Gf VII-X with values of 100–330 m in c. 4.5 Ma (~22–73 Mm*a^{-1}) in the basin centre. Again, erosion following Gf X and local structural overprint reduced the original thickness and, consequently, the subsidence rate.

Discussion

Comprehensive field data and a synthesis of published and unpublished information give a detailed view on an inner shelf basin of Baltica as distinct, and separated from, the outer shelf. The palinspastic restoration reveals an early Cambrian basin, defined here as Hornavan–Vattudal basin (HVB). It comprises the allochthonous Gärdsjön formation (Gf I-X) and the autochthonous Laisberg and Grammajukku formations (equivalent with Gf VI-X). The discussion puts the HVB, its geometry, sedimentary record, and tectonic evolution into the wider context of the Baltica–Iapetus passive margin and the foreland of the Timan orogen. Apart from the regional significance, the present example is of general importance for the structure of continental margins.

Restoration of the early Cambrian Hornavan–Vattudal basin (HVB)

The restoration of the HVB in the Lower Allochthon thrust nappes (Figs. 5, 6) is based on the observation of forward propagating thrusts during orogenic shortening. Recent age data from Træna and the Høgtuva-Sjona basement windows, at the Norwegian coast to the west of the Nasafjället window, suggest Caledonian, thrust-related deformation as early as c. 434 Ma (Schilling et al. 2015). In the west of the southern traverse, Bender et al. (2019) interpreted age data on mylonites of c. 435 to 426 Ma to reflect the ESE transport of the Caledonian nappe pile. Subsequent ESE-directed thrusting in the marginal thrust systems of the Lower Allochthon took place successively further towards the foreland in the east from c. 430 to 424 Ma (Greiling et al. 2013; Grimmer et al. 2015; and references therein), thus documenting an ESE, forward propagating orogenic wedge. Accordingly, the western successions, now in the western windows, were thrusted first and, consequently, restore to the west of the eastern, marginal thrust systems (Figs. 5,6). This age sequence supports the models of Hossack and Cooper (1986) and Rice and Anderson (2016), which put the basement windows originally in the west of the Lower Allochthon nappes at the Caledonian margin. The present observations in the Børgefjellet, Bångonåive, and Nasafjället windows of increasing stratigraphic range and thickness eastwards, towards an HVB depocenter further east (Fig. 4b, 7), provide a further, independent argument for this position. Together with the section-balancing data, this evidence indicates the windows contain the western HVB margin towards

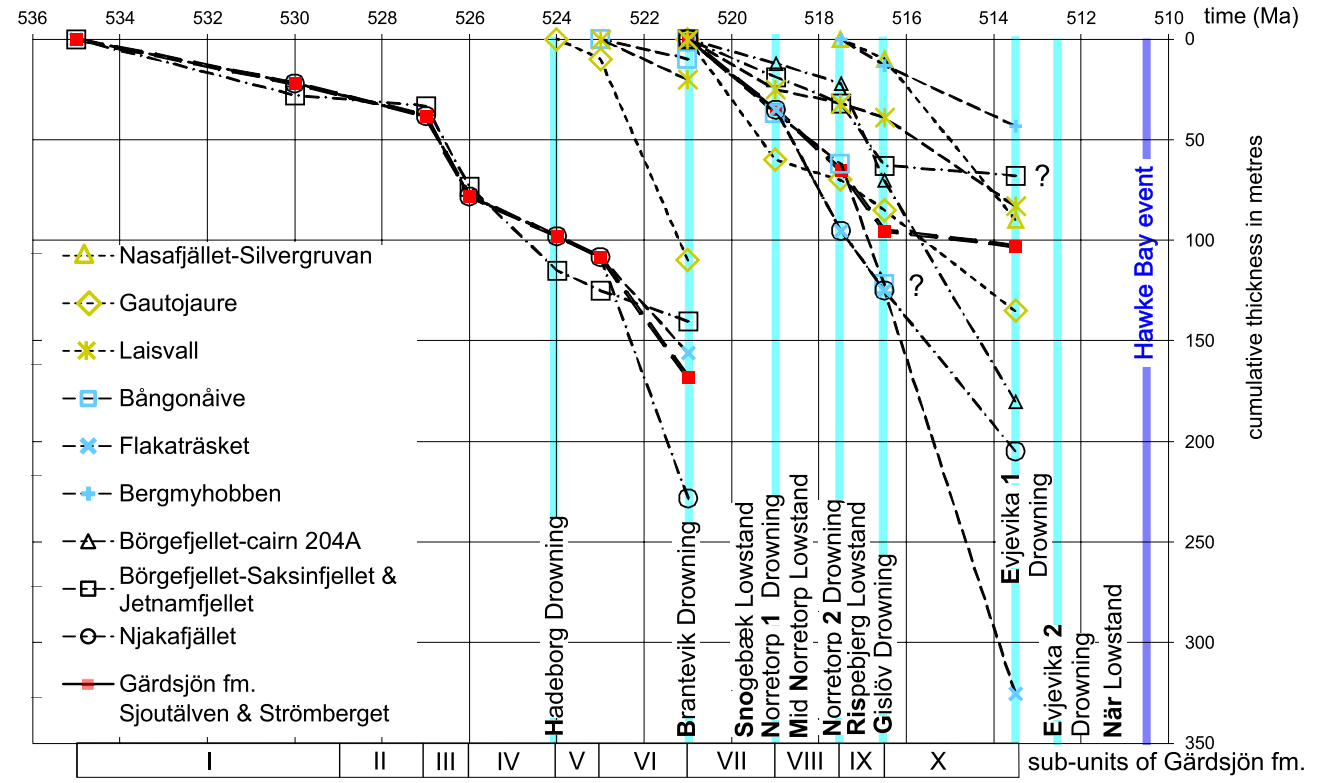

Fig. 10 Thickness versus age curves derived from the stratigraphic columns of Fig. 4. Drowning events (light blue vertical lines) from Nielsen and Schovsbo 2011; compare Fig. 9. Question marks refer to probable structural excision of parts of Gf X, bold letters to abbreviations in Fig. 9

a basement high in the west. Thus, this evidence rules out a simple geometry of an oceanward thickening shelf succession at the Baltica–Iapetus margin in early Cambrian times, as suggested by the traditional models for the central Scandinavian Caledonides (e.g. Nielsen and Schovsbo 2011; Gee and Stephens 2020).

Instead, the lower Cambrian HVB developed to the east of the basement highs in the windows with > 440 km in NE–SW direction and up to 330 km NW–SE (Figs. 6, 7). In the southwest, the HVB terminates against the GOC or the ODZ (Bergman and Sjöström 1994), where the cover is restricted to Gf X and only a few tens of metres thick (Gee 1974; Walser 1980; Lindqvist and Johansson 1987). Towards northeast, the sub-units terminate successively northwards from Flakaträsket via Gautojaure to Hornavan (Fig. 7) with the ATC further north as ultimate boundary. There again, the cover is restricted to Gf X. The eastern margin of the HVB is oriented SW–NE, obliquely across the present erosional margin of the Cambrian beds (SSW–NNE), controlled by local extensional fractures. Around Lake Storuman, ESE–WNW-trending (half-) graben structures intersect this margin (Fig. 6b). A high area oriented in the same direction stretches from Rönnberget to Stuphällan, at the southern side of Lake Vojmsjön (Fig. 6b; Greiling et al. 1996; Zachrisson and Greiling 1996). In a strip of a similar orientation south of the Nasafjället window, Cambrian beds are missing (Figs. 6, 11). There is no information, whether this is due to a similar high or a subsequent removal of beds.

Sedimentary record and basin evolution

In the HVB floor, the carbonates of the Risbäck group and glaciogenic diamictites of the Långmarkberg formation, related to the Marinoan glacial event at c. 635 Ma (Fig. 9), still covered the crystalline basement rocks at the onset of early Cambrian sedimentation, at least in the central and southern parts of the HVB (Fig. 3). Since these diamictites are widespread from southwestern to northern Scandinavia, their absence around Gautojaure and across ATC and GOC is probably not primary but due to erosion prior to Cambrian sedimentation. This is consistent with frequent traces of palaeoweathering in the HVB floor (e.g. Willdén 1980; Thelander 1982; Angerer and Greiling 2012; SI Fig. S2a), indicating a subaerial environment. In addition, components in the basal conglomerates of units Gf I-V indicate erosion of mostly Risbäck group arkoses and crystalline rocks. Recent reviews by Nielsen and Schovsbo (2011) and McLoughlin et al. (2021), together with age data from Peng et al. (2021) suggest a time at around 535 Ma for the onset of early Cambrian sedimentation in the HVB (Figs. 9, 10). There is thus

no sedimentary record documenting the c. 100 Ma interval after the deposition of diamictites of the Långmarkberg formation.

The early HVB sedimentation succeeds or accompanies extensional fracturing in the crystalline basement at c. 544–534 Ma (e.g., Billström et al. 2012; Saintilan et al. 2017), which probably created space for the HVB deposits. Diamictites at the base of Gf VI represent products of terrestrial erosion (Nielsen & Schovsbo 2011) and suggest emergence during a low stand, followed by Brantevik drowning and deposition of green shales with red layers and subordinate light-grey quartz arenite interlayers. These extended northwards to Bångonåive, Gautojaure, and Laisvall (Figs. 6, 7). Characteristic red interlayers occur in the southern part only (Fig. 6a). Minor channels at the top (SI Fig. S6e, f) suggest emergence and erosion after the deposition of Gf VI. Subsequent Norretorp 1 drowning, a coastal onlap of global distribution (Fig. 9), extends the basin into further parts of the Börgefjellet area. Basal diamictites there (SI Fig. S8f-h) and in the Bångonåive area (Greiling et al. 1993) indicate proximity to the western basin margin. In the Njakafjället area, their equivalents are basal conglomerates (SI Fig. S6d–f), probably shed from a local high (Stuphällan area). The related Gf VII deposits show sediment transport from the west, both at Laisvall and at Torneträsk (Willdén 1980; Thelander 1982), indicating a high area in the west (Fig. 6b). Syn-sedimentary normal faults with NNE–SSW-directed extension (Fig. 8) accompany the subsequent sedimentation. The Rönnberget–Stuphällan area, where the sedimentary record is restricted to Gf VIII–IX, may have persisted as a high until the deposition of Gf VIII, or faulting may have caused uplift and erosion of older Cambrian beds. In the Nasafjället area, Gf IX is the lowermost unit. Gf IX sediment transport is towards western and northern directions (Fig. 6b). Finally, Gf X shales, siltstones, and subordinate quartz arenites overstep the whole of the basin and also cover the ATC and GOC. The hiatus following Gf X until the onset of Alum shale formation sedimentation (c. 511–507 Ma) is time-related with a greenhouse climate from 514 to 509 Ma (Hearing et al. 2018).

Quartz arenites and their sedimentary structures such as cross-bedding and ripple marks (SI Fig. S4–6, 8c), indicate shallow water, mostly tidal zone, for most of the Gf. Where available, data on current directions suggest mostly E–W-directed sedimentary transport (SI Fig. S3a). The characteristic red interlayers of Gf VI do not extend into the near shore area at Laisvall (Willdén 1980; Fig. 6a), implying that they are restricted to deeper water. Load casts in Gf VIII (Gee et al. 1990) and graded beds in Gf IX at Bångonåive (Stephens 1977) suggest water levels below wave base. At the top of Gf X, phosphorite-bearing carbonates and conglomerates may indicate emergence and shallow water conditions (e.g. Bjørlykke et al. 2021). Alternatively, if a greenhouse climate produced a high sea level, these rocks may be products of submarine erosion, for example contourites (Wallin 1989).

The Cambrian beds to the north of the ATC show detrital zircon ages as young as Ediacaran and earliest Cambrian (Andresen et al. 2014; McLoughlin et al. 2021), which can be related to the Timan orogen in the north. In contrast, detrital zircons of the HVB are of Meso- and Palaeoproterozoic age with a few older ones (Gee and Stephens 2020; Fig. 11a). Apparently, the ATC acted as a barrier against zircons shed from the Timan foreland in the north. Towards south, the GOC with the ODZ may also have been a barrier against Neoproterozoic detrital zircons, which were deposited in SW Scandinavia beyond an "earliest Cambrian catchment divide" (Lorentzen et al. 2020; Fig. 11a: Hedmark basin). Further towards the southeast, detrital zircon ages of c. 530 Ma relate to Cadomian tectonic activity (Żelaźniewicz et al. 2020; Fig. 1a).

Tectonic evolution at the Baltica passive margin and the Timan foreland in early Cambrian times

The c. 596 Ma Ottfjället dykes (Kumpulainen et al. 2021) and their equivalents represent the youngest traces of rifting in the area (Fig. 9). Regionally, the Baltica–Iapetus rift–drift transition ended between 570 and 550 Ma (Li et al. 2008; Pease et al. 2008). At 544 to 534 Ma, normal faults document E–W extension (Billström et al. 2012; Saintilan et al. 2015; 2017) at the eastern margin of the incipient HVB. Around Laisvall, re-activation of basement fractures occurred at c. 521–514 Ma (Saintilan et al. 2015). Syn-depositional faults at Lake Vojmsjön formed at c. 519–517.5 Ma (Gf VII–VIII) and their geometry reflects E-W and NW–SE extension (Fig. 8a). At around 516 Ma (Gf IX–X), clastic dykes in the basement and normal faults (Fig. 8b-d) document extension in NNE–SSW direction at Lake Storuman. Observed extensional faults relate to thickness variations in the Storuman area (SI Fig. S3b), at Björnide (Sveriges geologiska undersökning 2020), and at Lake Hornavan (Kathol et al. 2012; Fig. 3). Varying thicknesses of Gf X (516.5–513.5 Ma) may indicate syn-depositional extension at Vietas and Laisvall (Hansen 1989; Saintilan et al. 2015). Low subsidence values during early deposition (Gf I-VI; Fig. 10) are consistent with thermal subsidence following early extension. Relatively rapid subsidence from 521 to 513.5 Ma (Gf VII–X), together with syn-sedimentary normal faults displacing Gf VII–IX (Fig. 8, SI Fig. S3b, 4b), indicate renewed tectonic activity.

The Baltica passive margin in the central to north-central parts of the Scandinavian Caledonides shows a more or less extended basement overlain by Neoproterozoic syn-rift sedimentary rocks, related to Rodinia break-up and Iapetus formation (e.g. Gee and Stephens 2020; Fig. 11). Towards the

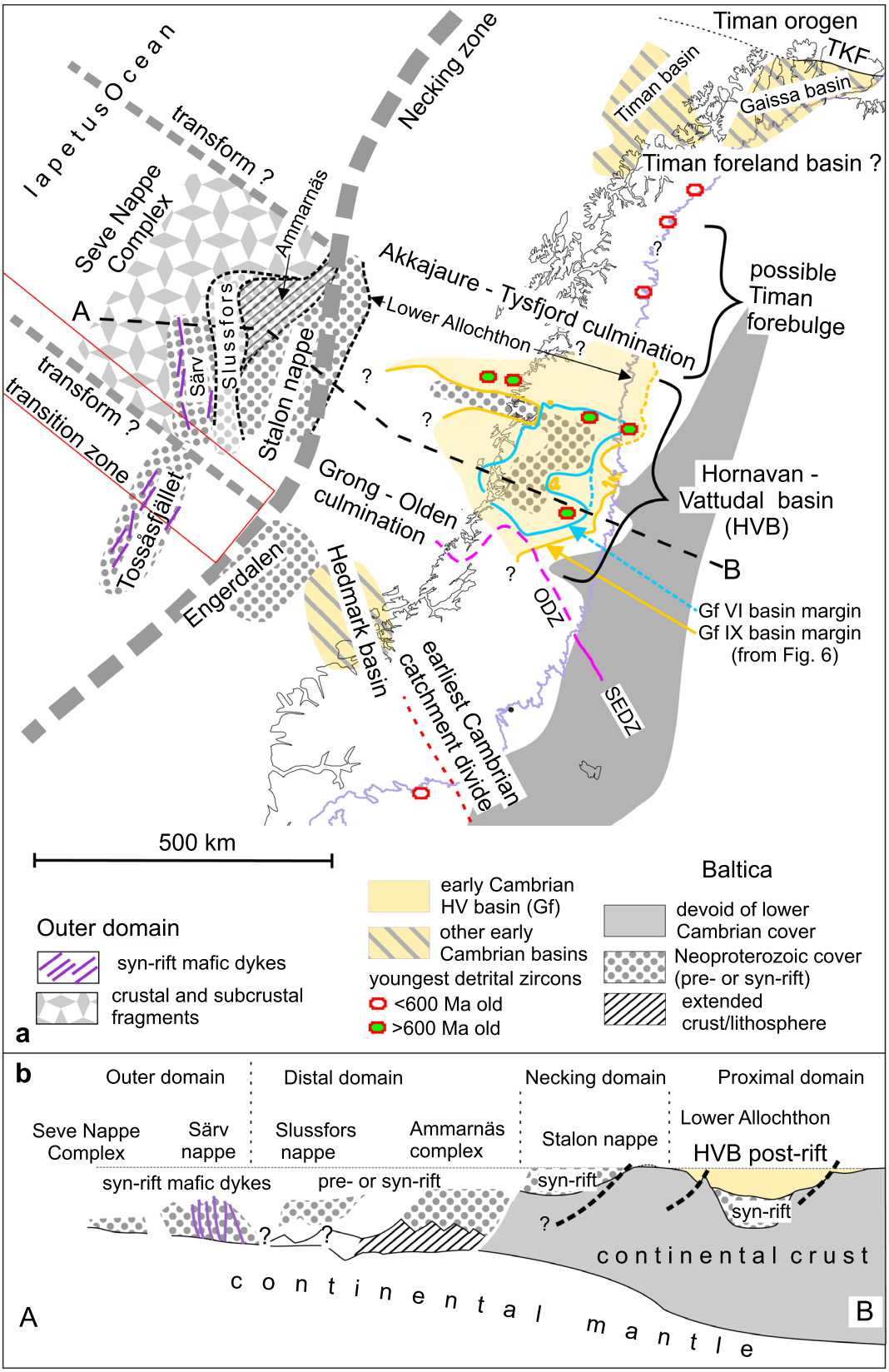
Iapetus Ocean
transform ?
Necking zone
Timan orogen
TKF
Timan basin
Gaissa basin
Timan foreland basin ?
Seve Nappe Complex
Ammarnäs
Akkajaure - Tysfjord culmination
possible Timan forebulge
A
Lower Allochthon
Särv
Slussfors
Stalon nappe
transform ?
transition zone
Grong - Olden culmination
Hornavan - Vattudal basin (HVB)
Tossåsfjället
Engerdalen
Hedmark basin
ODZ
B
Gf VI basin margin
Gf IX basin margin
(from Fig. 6)
earliest Cambrian catchment divide
SEDZ
500 km
Baltica
Outer domain
syn-rift mafic dykes
crustal and subcrustal fragments
early Cambrian HV basin (Gf)
other early Cambrian basins
youngest detrital zircons
<600 Ma old
>600 Ma old
devoid of lower Cambrian cover
Neoproterozoic cover (pre- or syn-rift)
extended crust/lithosphere
a
b
Outer domain
Distal domain
Necking domain
Proximal domain
Seve Nappe Complex
Särv nappe
Slussfors nappe
Ammarnäs complex
Stalon nappe
Lower Allochthon
HVB post-rift
syn-rift mafic dykes
pre- or syn-rift
syn-rift
syn-rift
continental crust
continental mantle
A
B

◂**Fig. 11** **a** Palaeogeographic situation of the HVB within the western Baltica passive margin towards the Iapetus Ocean, modified from Jakob et al. (2019; including "transition zone") and the present data, location on Fig. 1a. Gaissa and Timan basins and Trollfjorden–Komagelva Fault (TKF) simplified from Rice (2014) and Rice and Anderson (2016), Hedmark basin and "earliest Cambrian catchment divide" modified from Lorentzen et al. (2020). ODZ: Olden Discontinuity Zone, SEDZ: Storsjön–Edsbyn Deformation Zone (Bergman and Sjöström 1994; Bergman et al. 2006). Minor basins not shown. Line A–B shows approximate position of section in b). **b** Lithospheric section of a passive margin (simplified from McClay and Hammerstein 2020), adapted to the present area, with the tectonic position of the HVB

outer Baltica margin, Jakob et al. (2019) and Andersen et al. (2022) showed exposure of lower crustal and upper mantle rocks as traces of hyperextension in the present Lower and Middle Allochthons. In the Ammarnäs complex (Middle Allochthon, Fig. 11), c. 25% of crystalline basement rocks have mafic–ultra-mafic composition (Greiling et al. 2021), probably indicative of an extended lithosphere. The Särv nappe may contain up to 50% of dyke material (Gee and Kumpulainen 1980), which implies further crustal extension. The Seve nappes with abundant mafic and ultra-mafic rocks document even further extension, probably similar with the extensional allochthon of Jacob et al. (2019). In contrast, the HVB rests on a relatively little extended lithosphere between the hyper-extended margin in the W and the undeformed continent.

Basement highs delimit the HVB towards S (GOC), W (Børgefjellet, Bångonåive, Nasafjället), and N (ATC). Shape, size and tectonic evolution of the HVB compares well with other basins situated in the inner part of recent passive margins, for example the Vøring basin (e.g. Færseth 2020), SE Brazil (Silva and Sacek 2019), the Red Sea (Stockli and Bosworth 2019), and central Atlantic (Duval-Arnould et al. 2021). These basins are controlled by mostly margin-parallel faults and subordinate transverse structures at a high angle to the margin. An example for the latter, the GOC continues into a transition zone between magma-poor and magma-rich hyper-extended margins (Jacob et al. 2019; Andersen et al. 2022), which may be related to transform faults in the oceanic realm (Le Pouriet et al. 2017). Further work will have to show possible genetic relationships between GOC uplift and transform faulting. The margin-parallel basement high delimiting the HVB towards W may reflect footwall uplift, related to Cambrian age normal faults (Fig. 11b). Since it is close to the lithospheric necking zone as located by Jacob et al. (2019), lithospheric necking may have contributed to the uplift. Towards the north, the zircon record suggests the ATC as a divide between HVB and basins in the north (Timan, Gaissa basins, Rice and Anderson 2016) with input from the Timan orogen (e.g. Andresen et al. 2014; McLoughlin et al. 2021; Meinhold et al. 2022) during early Cambrian sedimentation. From Vietas, where only Gf X is present at the crest of the ATC (Fig. 7, Sect. 4), lower Cambrian beds are thickening northwards (e.g. Bergström and Gee (1985) and show the ATC as a physical barrier. As the GOC, the ATC may also be related with transform faults offshore. In contrast to the GOC, there is no support in the oceanic realm (e.g. Andersen et al. (2022) for such an interpretation. Alternatively, the ATC may be a forebulge related to compression in the Timan foreland. Compression or transpression by the Timan orogen (e.g. Gabrielsen et al. 2022), with a possible backstop at the southeast Baltica margin during early Cadomian collision (Żelaźniewicz et al. 2021), is consistent with WNW-directed "escape" towards the open face of the Iapetus Ocean in the west, along the observed normal faults (Figs. 3, 8). Subsequent WNW–ESE faults indicate NNE-directed extension after c. 516 Ma. This extension may be related to the incipient late-orogenic collapse in the Timan orogen, where uplift, erosion, and subsequent sedimentation occurred at least since mid-Cambrian times (e.g. Bogolepova and Gee 2004).

Supplementary Information The online version contains supplementary material available at https://doi.org/10.1007/s00531-023-02353-y.

Acknowledgements The work benefitted from the long and successful cooperation with numerous colleagues from the Geological Survey of Sweden in Uppsala, in particular Stefan Bergman and, earlier, Ebbe Zachrisson and Thomas Eliasson, which is gratefully acknowledged. Regional information includes data from numerous student theses from Heidelberg University and KIT, Karlsruhe, supervised by the first author, assisted by Jens Grimmer (KIT), who also contributed further data. The authors would like to thank Per-Gunnar Andréasson (Lund), Sören Jensen (Badajoz), and Axel Müller (Oslo) for discussions. Very thorough and constructive reviews by Sören Jensen and Hugh Rice, together with further suggestions by topical editor Guido Meinhold, helped to considerable improve the manuscript. The authors extend their sincere thanks. We acknowledge support by the KIT-Publication Fund of the Karlsruhe Institute of Technology.

Funding Open Access funding enabled and organized by Projekt DEAL. Authors were funded by their respective home institutions. There were no further sources of funding. There are no financial or non-financial interests that are directly or indirectly related to this work.

Availability of data and materials All data are available within this article and its supplementary material.

Declarations

Conflict of interest The authors declare that there is no conflict of interest.

References

Andersen TB, Jakob J, Kjøll HJ, Tegner C (2022) Vestiges of the pre-caledonian passive margin of baltica in the scandinavian caledonides: overview, revisions and control on the structure of the mountain belt. Geosciences 12:57. https://doi.org/10.3390/geosciences12020057

Andresen A, Agey-Dwarko NY, Kristoffersen N, Hanken NM (2014) A Timanian foreland basin setting for the late neoproterozoic-early Palaeozoic cover sequences (Dividal Group) of northeastern Baltica. Geol Soc London Spec Publ 390:157–175

Angerer T, Greiling RO (2012) Fabric evolution at basement-cover interfaces in a fold-and-thrust belt, and implications for décollement tectonics (Autochthon, Blaik Nappes, central Scandinavian Caledonides). Int J Earth Sci 101:1763–1788. https://doi.org/10.1007/s00531-012-0765-4

Bender H, Glodny J, Ring U (2019) Absolute timing of Caledonian orogenic wedge assembly, Central Sweden, constrained by Rb–Sr multi-mineral isochron data. Lithos 344–345:339–359

Bergman S, Kathol B (2018) Synthesis of the bedrock geology in southern Norrbotten county, northern Sweden. Sver Geol Unders Rapporter Och Meddelanden 144:243

Bergman S, Sjöström H (1994) The Storsjön-Edsbyn Deformation Zone, central Sweden. Institute of Earth Sciences Uppsala University:46p. https://uu.diva-portal.org/smash/record.jsf?pid=diva2%3A1148457&dswid=-8251

Bergman S, Sjöström H, Högdahl K (2006) Transpressive shear related to arc magmatism: the Paleoproterozoic Storsjön-Edsbyn deformation zone, central Sweden. Tectonics. https://doi.org/10.1029/2005TC001815

Bergman S, Stephens MB, Anderson J, Kathol B, Bergman T (2012) Bedrock map of Sweden, scale 1:1 million. Sver geol unders K 423. http://resource.sgu.se/produkter/k/k423-karta.pdf

Bergström J, Gee DG (1985) The Cambrian in Scandinavia. In Gee DD, Surt BA (eds) The Caledonide Orogen-Scandinavia and Related Areas: 247–271.

Bierlein F-P, Greiling RO (1993) New constraints on the basal sole thrust at the eastern Caledonian margin in northern Sweden. Geol Fören Stockh Förh 115:109–116

Billström K, Broman C, Schneider J, Pratt W, Skogsmo G (2012) Zn-Pb ores of Mississippi valley type in the Lycksele-Storuman district, Northern Sweden: a possible rift-related Cambrian mineralisation event. Minerals 2:169–207. https://doi.org/10.3390/min2030169

Björk L, Kero L, Zachrisson E (1996) Bedrock map 22G Vilhelmina SO, 1:50 000. Sver geol unders Ai 87.

Björklund L (1989) Geology of the Akkajaure-Tysford-Lofoten traverse, N. Scandinavian Caledonides. Geol Inst Publ A 59:244p. https://gupea.ub.gu.se/handle/2077/15375

Bjørlykke A, Lepland A, Skår Ø (2021) Origin of the mineralised Hawke Bay conglomerate and its importance in formation of the Vassbo lead-zinc deposit. Sweden Norw J Geol 101:202109. https://doi.org/10.1785/njg101-2-4

Bogolepova OK, Gee DG (2004) Early Palaeozoic unconformity across the Timanides, NW Russia. In: Gee DG, Pease V (eds) The Neoproterozoic Timanide Orogen of Eastern Baltica. Early Palaeozoic unconformity across the Timanides, NW Russia. Geol Soc London, Mem. 30:145–157.

Cederström P, Geyer G, Ahlberg P, Nilsson CH, Ahlgren J (2022) Ellipsocephalid trilobites from Cambrian Series 2 and Stage 4, with emphasis on the taxonomy, morphological plasticity and biostratigraphic significance of ellipsocephalids from Scania, Sweden. Fossils Strata 67:1–131

Davis D, Suppe J, Dahlen A (1983) Mechanics of fold-and-thrust belts and accretionary wedges. J Geophys Res 88(B2):1153–1172

Dewey JF, Strachan RA (2003) Changing Silurian–Devonian relative plate motion in the Caledonides: sinistral transpression to sinistral transtension. J Geol Soc London 160:219–229. https://doi.org/10.1144/0016-764902-085

Dohme G, Greiling R (1981) Structure of the Bångfjället complex as indicated by geological and geophysical data. Earth Evolution Sci 1:38–42

Du Rietz T (1960) Tectonic conditions in the Front Range of the Swedish Caledonian in Central Norrland. Sver geol unders C 568:57 p. https://resource.sgu.se/dokument/publikation/c/c568rapport/

Duval-Arnould A, Schröder S, Charton R, Joussiaume R, Razin P, Redfern J (2021) Early post-rift depositional systems of the Central Atlantic: lower and middle Jurassic of the Essaouira-Agadir Basin. Morocco J African Earth Sci 178:104164

Eliasson T, Greiling RO, Triumf CA-A (2001) Bedrock map 23H Stensele NV, 1:50 000. Sver geol unders Ai 126. https://resource.sgu.se/dokument/publikation/ai/ai126karta/

Eliasson T, Greiling RO, Triumf CA-A (2003) Bedrock maps 24H Sorsele NV, SV, 1:50 000. Sver geol unders Ai 187, 188. https://resource.sgu.se/dokument/publikation/ai/ai187karta/

Færseth RB (2020) Structural geology and basin development of the Norwegian Sea. Norwegian J Geol. 100:202018. https://doi.org/10.17850/njg100-4-1

Febbroni S (1997) Rilevamento geologico e dei valori della suscettività magnetica nelle Caledonidi della Lapponia svedese. AZ Marmi 131:50

Foslie S, Strand T (1956) Namsvatnet med en del av Frøyningsfjell. Norges Geol Unders 196:1–82

Gabrielsen RH, Roberts D, Gjelsvik T, Sygnabere TO, Hassaan M, Faleide JI (2022) Double-folding and thrust-front geometries associated with the Timanian and Caledonian orogenies in the Varanger Peninsula, Finnmark North Norway. J Geol Soc 179:2022. https://doi.org/10.1144/jgs2021-153

Gayer RA, Greiling RO (1989) Caledonian nappe geometry in north central Sweden and basin evolution on the Baltoscandian margin. Geol Mag 126:499–513

Gee DG (1974) Comments on the metamorphic allochthon in northern Trøndelag, central Scandinavian Caledonides. Norsk Geol Tidsskr 54:435–440

Gee DG, Kumpulainen R (1980) An excursion through the Caledonian mountain chain in central Sweden from Östersund to Storlien. Sver Geol Unders C 774:1–66

Gee DG, Stephens MB (2020) Lower thrust sheets in the Caledonide orogen, Sweden: Cryogenian-Silurian sedimentary successions and underlying, imbricated, crystalline basement. Geol Soc London Mem 50:495–515. https://doi.org/10.1144/M50-2018-7

Gee DG, Kumpulainen R, Thelander T (1978) The Tåsjö decollement, central Swedish Caledonides. Sver geol unders C742:35 p. https://resource.sgu.se/dokument/publikation/c/c742rapport

Gee DG, Kumpulainen R, Karis L (1990): Fjällrandens berggrund. In: Lundqvist, T., Beskrivning till berggrundskartan över Västernorrlands Län. Sver geol unders Ba 31:206–237.

Geyer G (2019) A comprehensive Cambrian correlation chart. Episodes 42:321–332. https://doi.org/10.18814/epiiugs/2019/019026

Gjelle S (1988) Geologisk kart over Norge, berggrunnskart Saltdal, M 1:250 000. Norges geol unders, Trondheim. https://aps.ngu.no/pls/oradb/rf.Visdok?c_dokid=0000036826

Grambow C (2001) Das Råvovare-Konglomerat: Geologischer Rahmen und regionale Vergleiche (Kaledoniden in Västerbotten, Schweden) kombiniert mit einer Kartierung der umgebenden Gesteine

des Unteren-, Mittleren- und Oberen Allochthons. Diplomarbeit, Ruprecht-Karls-Univ Heidelberg: 111
Greiling R (1972) Geologie des östlichsten Teils des Børgefjell-Fensters in den nördlichen Kaledoniden Skandinaviens. Diplomarbeit, Philipps-Univ Marburg: 97
Greiling RO (1981) Caledonian thrusting in the basement rocks of the Børgefjell window (north-central Scandinavian Caledonides) as related to major nappe transport. Terra Cognita 1:47
Greiling R (1985) Strukturelle und mctamorphe Entwicklung an der Basis grosser, weittransporticrtcr Deckeneinhciten am Beispiel des Mittlcrcn Allochthons in den zentralcn Skandinavischen Kaledonidcn (Stalon-Dcckcnkomplex in Västcrbottcn, Schweden). Geotekt Forsch 69:1–129
Greiling RO (1988) Ranseren Berggrunnskart 2025 3, 1:50.000, foreløpig utgave. Norges Geol unders, Trondheim. https://aps.ngu.no/pls/oradb/rf.Visdok?c_dokid=0000036619
Greiling RO, Garfunkel Z (2007) An early Ordovician (Finnmarkian?) foreland basin and related lithospheric flexure in the Scandinavian Caledonides. Am J Sci 307:527–553
Greiling RO, Kathol B (2021a) Description to the Bedrockmaps 25G Ammarnäs NV, NO, SV & SO, 1:50.000. Sver geol unders K 690:57p. https://resource.sgu.se/dokument/publikation/k/k690beskrivning/
Greiling RO, Kathol B (2021b) Bedrockmap 25G Ammarnäs SO, 1:50.000. Sver geol unders K 682 https://resource.sgu.se/dokument/publikation/k/k682karta/
Greiling RO, Kathol BK (2021c) Description to the bedrock maps 24G Umnäs NV, NO, SV & SO, 1:50.000. Sver geol unders K 712:61p. http://resource.sgu.se/dokument/publikation/k/k712beskrivning/k712-beskrivning.pdf.
Greiling RO, Kathol BK (2021d) Bedrock maps 24G Umnäs NV, NO, SV, SV, 1:50 000. Sver geol unders K 706, 707, 708, 709. http://resource.sgu.se/dokument/publikation/k/k706karta/k706-karta.pdf.
Greiling RO, Zachrisson E (1999) Bedrockmaps 23 G Dikanäs NV, SV, 1:50.000. Sver geol unders Ai 122, 123. https://resource.sgu.se/dokument/publikation/ai/ai122karta/ai122-karta.pdf.
Greiling RO, Gayer RA, Stephens MB (1993) A basement culmination in the Scandinavian Caledonides formed by antiformal stacking (Bångonåive, northern Sweden). Geol Mag 130:471–482
Greiling RO, Zachrisson E, Björk L, Kero L (1996) Bedrockmap 22 G Vilhelmina NO, 1:50.000. Sver geol unders Ai 86. http://resource.sgu.se/dokument/publikation/ai/ai86karta/ai86-karta.pdf
Greiling RO, Garfunkel Z, Zachrisson E (1998) Evolution of the orogenic wedge in the central Scandinavian Caledonides and its interaction with the foreland lithosphere. GFF 120:181–190
Greiling RO, Zachrisson E, Thelander T, Sträng T (1999) Bedrockmaps 23 G Dikanäs NO, SO, 1:50.000. Sver geol unders Ai 124, 125. https://resource.sgu.se/dokument/publikation/ai/ai124karta/pdf.
Greiling RO, Grimmer JC, de Wall H, Björk L (2007) Mesoproterozoic dyke swarms in foreland and nappes of the central Scandinavian Caledonides: structure, magnetic fabric, and geochemistry. Geol Mag 144:525–546. https://doi.org/10.1017/S0016756807003299
Greiling RO, Oszczypko N, Garfunkel Z (2013) A comparison of two orogenic margins: central Scandinavian Caledonides and western Outer Carpathians. Z Dt Ges Geowiss (german J Geosci) 164:9–32. https://doi.org/10.1127/1860-1804/2013/0013
Greiling RO, Kathol B, Kumpulainen RA (2018) Nappe units along the Caledonian margin in central Scandinavia (Grong-Olden to Nasafjället): definition, distinction criteria, and tectonic evolution. GFF 140:66–89. https://doi.org/10.1080/11035897.2018.1453864
Greiling RO, Grimmer JC, Kathol B (2021) Bedrockmaps 25G Ammarnäs, 1:50.000 NO, NV SV. Sver Geol Unders K 681(683):684
Grimmer JC, Greiling RO (2004) Neoproterozoic to Ordovician passive margin of Baltoscandia: restoration of basin geometry and Caledonian structural evolution (central Swedish Caledonides). Réunion des Sciences de la Terre—Joint Earth Sciences Meeting, Strasbourg, abstract on CD.
Grimmer JC, Glodny J, Drüppel K, Greiling RO, Kontny A (2015) Early- to Mid-Silurian extrusion wedge tectonics in the central Scandinavian Caledonides. Geology 43(4):347–350. https://doi.org/10.1130/G36433.1
Gustavson M (1973) Børgefjell. Beskrivelse til det berggrunnsgeologiske gradteigskart J.19 1:100 000. Norges Geologiske Undersøkelse 298:1–43. https://aps.ngu.no/pls/oradb/rf.Visdok?c_dokid=0000036176
Hansen L (1989) Age relationships between normal and thrust faults near the Caledonian Front at the Vietas Hydropower Station, northern Sweden. In: Gayer RA (ed), The Caledonide Geology of Scandinavia. (Graham and Trotman) London:91–100.
Hansson KE (1977) Kvartsit vid Hornavan. Examensarbete, Högskolan i Luleå 77(066E):85p
Hearing TW, Harvey THP, Williams M, Leng MJ, Lamb AL, Wilby PR, Gabbott SE, Pohl A, Donnadieu Y (2018) An early Cambrian greenhouse climate. Sci Adv 4(5):eaar5690. https://doi.org/10.1126/sciadv.aar5690
Hossack JR, Cooper MA (1986) Collision tectonics in the Scandinavian Caledonides. In: Coward MP, Ries AC (eds), 1986, Collision Tectonics, Geol Soc Spec Publ 19:287–304.
Jakob J, Andersen TB, Kjøll HJ (2019) A review and reinterpretation of the architecture of the South and South-Central Scandinavian Caledonides—a magma-poor to magma-rich transition and the significance of the reactivation of rift inherited structures. Earth-Sci Rev 192:513–528
Johansson Å (2014) From Rodinia to Gondwana with the 'SAMBA' model—a distant view from Baltica towards Amazonia and beyond. Precambrian Res 244:226–235
Kathol B, Weihed P (2005) Description of regional geological and geophysical maps of the Skellefte District and surrounding areas. Sver Geol Unders Ba 57:197
Kathol B, Sadeghi M, Triumf CA-A, Larsson D (2012) Berggrundsgeologisk undersökning, Jäkkvik-Boden. SGU-Rapport 2012(5):1–39
Kjøll HJ (2020) Late Neoproterozoic basin evolution of the magma-rich Iapetus margin of Baltica. Norw J Geol 100:202005. https://doi.org/10.17850/njg100-1-6
Kulling O (1942) Grunddragen av fjällkedjerandens bergbyggnad inom Västerbottens län. Sver geol unders C 445:320 p. https://resource.sgu.se/dokument/publikation/c/c445rapport/
Kulling O (1955) Den Kaledoniska fjällkedjans berggrund inom Västerbottens län. In Gavelin S, Kulling O (eds) Beskrivning till berggrundskarta över Västerbottens län. Sver geol unders Ca 37:101–296. https://resource.sgu.se/dokument/publikation/ca/ca55beskrivning/
Kumpulainen R (1982) The Upper Proterozoic Risbäck group, northern Jämtland and southwestern Västerbotten, central Swedish Caledonides. Univ Upps Dept Mineral Petrol Res Rep 28:60
Kumpulainen RA (2017) Guide for geological nomenclature in Sweden. GFF 139:3–20. https://doi.org/10.1080/11035897.2016.1178666
Kumpulainen R, Nystuen JP, Thelander T (1981) Late Precambrian stratigraphy (including tillies) within the Caledonian front from central-west Sweden to southeastern Norway. Upps Caled Symp Excursion B 8:76p
Kumpulainen RA, Hamilton MA, Söderlund U, Nystuen JP (2021) U-Pb baddeleyite age for the Ottfjället Dyke Swarm, central Scandinavian Caledonides: new constraints on Ediacaran opening of the Iapetus ocean and glaciations on Baltica. GFF 143:40–54. https://doi.org/10.1080/11035897.2021.1888314

Le Pourhiet L, May DM, Huille L, Watremez L, Leroy S (2017) A genetic link between transform and hyper-extended margins. Earth Planet Sci Lett 465:184–192. https://doi.org/10.1016/j.epsl.2017.02.043

Li ZX, Bogdanova SV, Collins AS, Davidson A, De Waele B, Ernst RE, Fitzsimons ICW, Fuck RA, Gladkochub DP, Jacobs J, Karlstrom KE, Lu S, Ntapov LM, Pease V, Pisarevsky SA, Thrane K, Vernikovsky V (2008) Assembly, configuration, and break-up history of Rodinia: a synthesis. Prec Res 160:179–210. https://doi.org/10.1016/j.precamres.2007.04.021

Lidmar-Bergström K, Olvmo M (2015) Plains, steps, hilly relief and valleys in northern Sweden—review, interpretations and implications for conclusions on Phanerozoic tectonics. Sver Geol Unders C 838:1–42

Lilljequist R (1973) Caledonian geology of the Laisvall area, southern Norrbotten Swedish Lapland. Sver Geol Unders C 691:1–43

Lindqvist J-E (1988) Tectonic implications of U-, Mo- and V-enriched graphitic phyllites in the Høgtuva and Nasafjäll Windows, Scandinavian Caledonides. Nor Geol Tidsskr 68:187–199

Lindqvist J-E, Johansson L (1987) Metamorphism and timing of thrusting in the Tømmerås Window, central Scandinavian Caledonides. Geol Fören Stockh Förh 109:35–146

Lorentzen S, Braut T, Augustsson CA, Nystuen JP, Jahren J, Schovsbo NH (2020) Provevenance of lower Cambrian quartz arenite on southwestern Baltica: weathering versus recycling. J Sed Res 90:493–512. https://doi.org/10.2110/jsr.2020.20

Marklund N (1952) A Cambro-Ordovician type-section in the Sarvas region S. E. of Nasafjäll, Lapland, and Problems suggested thereby. Geol Fören Stockh Förh 74:553–584

Mattern F, Scharf A, Al-Sarmi M, Pracejus B, Al-Hinaai A-S, Al-Mamari A (2018) Compaction history of Upper Cretaceous shale and related tectonic framework, Arabian Plate Eastern Oman Mountains. Arabian J Geosci 11(444):1–12. https://doi.org/10.1007/s12517-018-3781-2

McClay KR, Hammerstein JA (2020) Passive margins: tectonics, sedimentation and magmatism. Geol Soc London 476:1–9

McLoughlin S, Vajda V, Topper TP, Crowley JL, Liu F, Johansson O, Skovsted CB (2021) Trace fossils, algae, invertebrate remains and new U-Pb detrital zircon geochronology from the lower Cambrian Torneträsk Formation, northern Sweden. GFF 143:103–133. https://doi.org/10.1080/11035897.2021.1939775

Meinhold G, Willbold M, Karius V, Jensen S, Agić H, Ebbestad JOR, Palacios T, Högström AES (2022) Høyberget M Taylor, WM (2022) Rare earth elements and neodymium and strontium isotopic constraints on provenance switch and post-depositional alteration of fossiliferous Ediacaran and lowermost Cambrian strata from Arctic Norway. Prec Res 381:106845. https://doi.org/10.1016/j.precamres.2022.106845

Moczydłowska M, Jensen S, Ebbestad JOR, Budd GE, Martí-Mus M (2001) Biochronology of the autochthonous Lower Cambrian in the Laisvall-Storuman area, Swedish Caledonides. Geol Mag 138:435–453

Morley CK (1986) The Caledonian thrust front and palinspastic restorations in the southern Norwegian Caledonides. J Struct Geol 8:753–765

Nielsen AT, Schovsbo NH (2011) The Lower Cambrian of Scandinavia: depositional environment, sequence stratigraphy and palaeogeography. Earth-Sci Rev 107:207–310

Nielsen AT, Schovsbo NH (2015) The regressive Early-Mid Cambrian 'Hawke Bay event' in Baltoscandia: Epeirogenic uplift in concert with eustasy. Earth-Sci Rev 151:288–350

Nielsen AT, Ahlberg P (2019) The Miaolingian, a new name for the 'Middle' Cambrian (Cambrian Series 3): identification of lower and upper boundaries in Baltoscandia. GFF 141:162–173. https://doi.org/10.1080/11035897.2019.1621374

Osmundsen PT, Braathen A, Nordgulen Ø, Roberts D, Meyer GB, Eide E (2003) The Devonian Nesna shear zone and adjacent gneiss-cored culminations, North-Central Norwegian Caledonides. J Geol Soc London 160:137–150

Pease V, Dovzhikova E, Beliakova L, Gee DG (2004) Late Neoproterozoic granitoid magmatism in the basement to the Pechora Basin, NW Russia: geochemical constraints indicate westward subduction beneath NE Baltica. In Gee DG, Pease V (eds) The Neoproterozoic Timanide Orogen of Eastern Baltica. Geol Soc London, Mem 30:75–85.

Pease V, Daly JS, Elming S-Å, Kumpulainen R, Moczydlowska M, Puchkov V, Roberts D, Saintot A, Stephenson R (2008) Baltica in the Cryogenian, 850–630 Ma. Precambrian Res 160:46–65

Peng SCA, Babcock LE, Ahlberg P (2020) The Cambrian period. In: Gradstein FM, Ogg JG, Schmitz MD, Gradstein GM (eds) Geologic time scale. Elsevier, Amsterdam, pp 565–629

Rice AHN (2014) Restoration of the external caledonides, Finnmark, North Norway. In: Corfu F, Gasser D, Chew DM (eds) New perspectives on the caledonides of Scandinavia and related areas. Geol Soc London, Spec Publ, vol 390, pp 271–299. https://doi.org/10.1144/SP390.18

Rice AHN (2023) U-Pb baddeleyite age for the Ottfjället Dyke Swarm, central Scandinavian Caledonides: New constraints on Ediacaran opening of the Iapetus Ocean and glaciations on Baltica—a comment on the inferred age of Neoproterozoic glaciations. GFF. https://doi.org/10.1080/11035897.2023.2205893

Rice AHN, Anderson MW (2016) Restoration of the external Scandinavian Caledonides. Geol Mag 153:1136–1165. https://doi.org/10.1017/S0016756816000340

Ripa M, Stephens MB (2020) Dolerites, (1.27–1.25 Ga) and alkaline ultrabasic dykes (c. 1.14 Ga) related to intracrationc rifting. In: Stephens MB, Bergman Weihed J (eds) Sweden: Lithotectonic Framework, Tectonic Evolution and Mineral Resources. Geol Soc London, Mem. 50:315–323.

Romer RL, Bax G, Kathol B (1994) Basement control of the Caledonian orogen along the Torneträsk section, northern Sweden. Schweiz Mineral Petrogr Mitt 74:469–481

Saintilan NJ, Stephens MB, Lundstam E, Fontboté L (2015) Control of reactivated proterozoic basement structures on sandstone-hosted Pb-Zn deposits along the Caledonian Front, Sweden: evidence from airborne magnetic data, structural analysis, and ore-grade modeling. Econ Geol 110:91–117

Saintilan NJ, Stephens MB, Spikings R, Schneider J, Chiaradia M, Spangenberg JE, Ulianov A, Fontboté L (2017) Polyphase vein mineralization in the Fennoscandian Shield at Åkerlandet, Järvsand, and Laisvall along the erosional front of the Caledonian orogen, Sweden. Miner Deposita 52:823–844. https://doi.org/10.1007/s00126-016-0698-0

Schenk V (1975) Geologie der Kaledoniden am Hotagen See. Zentral-Schweden Sver Geol Unders C 715:43p

Schilling J, Bingen B, Skår Ø, Wenzel T, Markl G (2015) Formation and evolution of the Høgtuva beryllium deposit. Norway Contrib Mineral Petrol 170:30. https://doi.org/10.1007/s00410-015-1179-7

Silva RM, Sacek V (2019) Shallow necking depth and differential denudation linked to post-rift continental reactivation: the origin of the Cenozoic basins in southeastern Brazil. Terra Nova 31:527–533. https://doi.org/10.1111/ter.12423

Silvennoinen A, Gustavson M, Perttunen V, Siedlecka A, Sjöstrand T, Stephens MB, Zachrisson E (1987) Geological map, Pre-Quaternary rocks, Northern Fennoscandia. Scale 1:1 000 000. Geol Surv Finland Norway Sweden.

Slama J, Pedersen RB (2015) Zircon provenance of SW Caledonian phyllites reveals a distant Timanian sediment source. J Geol Soc 172:465–478. https://doi.org/10.1144/jgs2014-143

Solli A, Nordgulen Ø (2008) Bedrock map of Norway and the Caledonides in Sweden and Finland 1: 2 000 000. Norges geologiske undersøkelse, Trondheim, Norway.

Stålhös G (1958) Fjällrandens sparagmit- och kvartsitformationer—en petrografisk jämförelse. Geol Fören Stockh Förh 80:209–225

Stephens MB (1977) Stratigraphy and relationship between folding, metamorphism and thrusting in the Tärna-Björkvattnet area, northern Swedish Caledonides. Sver Geol Unders C 726:146

Stephens MB (2001) Bedrockmap 24F Tärna NO 1:50 000. Sver geol unders Ai 163.

Stockli DF, Bosworth W (2019) Timing of extensional faulting along the magma-poor central and northern Red Sea rift margin—transition from regional extension to necking along a hyperextended rifted margin. In: Rasul NM, Stewart ICF (eds) Geological setting, palaeoenvironment and archaeology of the Red Sea. Springer, Berlin, pp 81–111

Strand T, Kulling O (1972) Scandinavian caledonides. Wiley-Interscience, London, p 302

Sveriges geologiska undersökning (2020) Borrplats Björnide. https://apps.sgu.se/kartvisare/kartvisare-borrkarnor.html

Thelander T (1982) The Torneträsk Formation of the Dividal Group, northern Swedish Caledonides. Sver Geol Unders C 789:1–41

Thelander T (1994) The Laisvall and Grammajukku Formations (Dividal Group) of southern Norrbotten County. Sver Geol Unders BRAP 94009:64

Thelander T (2009) Beskrivning till berggrundskartan Kaledoniderna i norra Sverige. Sver Geol Unders K 222:1–51

Thelander T, Bakker E, Nicholson R (1980) Basement-cover relationships in the Nasafjäll Window, central Swedish Caledonides. Geol Fören Stockh Förh 102:569–580

Wallin B (1989) Origin of the Lower Cambrian phosphatic bed at Vassbo, Sweden. Terra Nova 1:274–279

Walser G (1980) Geology of the Hotagen area Jämtland central Sweden. Sver Geol Unders C 757:1–57

Warr LN, Greiling RO, Zachrisson E (1996) Thrust-related, very low-grade metamorphism in the marginal part of an orogenic wedge, Scandinavian Caledonides. Tectonics 15:1213–1229

Willdén MY (1980) Paleoenvironment of the autochthonous sedimentary rock sequence at Laisvall, Swedish Caledonides. Stockh Contrib Geol 33:1–100

Zachrisson E (1991) Bedrock maps 23E Sipmeke SV-SO, NO, 1:50 000. Sver geol unders Ai, 73, 74. https://resource.sgu.se/dokument/publikation/ai/ai73karta/ai73-karta.pdf

Zachrisson E (1997) Bedrock maps 22F Risbäck NV, NO, SV, SO, 1: 50 000. Sver geol unders Ai 102–105. https://resource.sgu.se/dokument/publikation/ai/ai102karta/ai102-karta.pdf

Zachrisson E, Greiling RO (1993) Bedrock maps 23 F Fatmomakke NO, SO, 1:50 000. Sver geol unders Ai 77, 78. https://resource.sgu.se/dokument/publikation/ai/ai77karta/ai77-karta.pdf

Zachrisson E, Greiling RO (1996) Bedrock map 22G Vilhelmina NV, 1:50 000. Sver geol unders Ai 84. http://resource.sgu.se/dokument/publikation/ai/ai84karta/ai84-karta.pdf

Żelaźniewicz A, Oberc-Dziedzic T, Slama J (2020) Baltica and the Cadomian orogen in the Ediacaran–Cambrian: a perspective from SE Poland. Int J Earth Sci. https://doi.org/10.1007/s00531-020-01858-0